

CFO Estimation for Massive MU-MIMO Systems

Sudarshan Mukherjee, *Student Member, IEEE*, and

Saif Khan Mohammed, *Member, IEEE*

Abstract

Low-complexity carrier frequency offset (CFO) estimation/compensation in massive multi-user (MU) multiple-input multiple-output (MIMO) systems is a challenging problem. The existing CFO estimation/compensation strategies for conventional small MIMO systems experience tremendous increase in complexity with increasing number of the user terminals (UTs), K and the number of base station (BS) antennas, M (i.e. in massive MIMO regime). In this paper, we devise a *low-complexity* algorithm for CFO estimation using the pilots received at the BS during a special uplink slot. The total per-channel use complexity of the proposed algorithm increases only linearly with increasing M and is independent of K . Analytical expression is derived for the mean square error (MSE) of the proposed CFO estimator. Further analysis reveals that the MSE of the proposed estimator decreases with increasing M (fixed K) and increasing K (fixed M and CFO pilot sequence length $\gg K$). We also derive an achievable information sum-rate expression of the time-reversal maximal-ratio-combining (TR-MRC) detector in the presence of residual CFO errors, resulting from the proposed CFO estimation/compensation algorithm. Analysis of this information rate expression reveals that an $\mathcal{O}(\sqrt{M})$ array gain is achievable. This new result is interesting since the best possible array gain under an ideal no CFO condition is also known to be $\mathcal{O}(\sqrt{M})$.

Index Terms

Massive MIMO, carrier frequency offset (CFO), multi-user, frequency-selective, low-complexity.

I. INTRODUCTION

In recent years, the evolution of wireless technology has felt the need for a paradigm shift in order to cope with the explosive growth in demand for mobile data traffic [1]. The need to support this tremendous increase in required data rate is the main driving force behind the

The authors are with the Department of Electrical Engineering, Indian Institute of Technology (I.I.T.) Delhi, India. Saif Khan Mohammed is also associated with Bharti School of Telecommunication Technology and Management (BSTTM), I.I.T. Delhi. Email: saifkhanmohammed@gmail.com. This work is supported by EMR funding from the Science and Engineering Research Board (SERB), Department of Science and Technology (DST), Government of India.

This paper is a substantial extension to the work submitted to IEEE Globecom 2015 [17].

evolution of the next generation 5G wireless systems [2]. The reduction in round-trip latency in communication networks and more efficient energy consumption are the other prime features that need to be addressed by the next generation 5G wireless systems. In the past few years, massive multiple-input multiple-output (MIMO) systems/large scale antenna systems (LSAS) have emerged as a potential 5G technology due to their ability to support high data rate and improved energy efficiency at relatively low implementation complexity [3]. In a multi-user (MU) massive MIMO system, the base station (BS) is equipped with hundreds of antennas to simultaneously communicate with only a few tens of single-antenna user terminals (UTs) in the same time-frequency resource [4]. Increase in the number of BS antennas opens up more available spatial degrees of freedom, enabling support to a large number of UTs and thus improving the achievable spectral efficiency [5], [6]. At the same time, the required radiated power can be scaled down for a fixed desired information rate, with increasing number of BS antennas, M [7]. Recent studies have revealed that even with imperfect channel state information (CSI), an $\mathcal{O}(\sqrt{M})$ array gain can be achieved while maintaining a fixed per-user information rate [8].

These results on massive MIMO systems however assume perfect frequency synchronization for coherent multi-user detection (MUD) at the BS. In practice, however achieving perfect frequency synchronization is challenging owing to the existence of carrier frequency offsets (CFOs) between the carrier frequency of the user signals received at the BS and the frequency of the BS oscillator. Without any estimation/compensation method, these CFOs can severely impact the performance of coherent MUD. In the past decade there have been numerous works reported on frequency synchronization in conventional small scale MIMO systems. The early works by Stoica and Besson paved the way to evaluating the Cramer-Rao lower bound (CRLB) for the best possible CFO estimate and its corresponding training sequence/pilot design [9], [10]. Their work has later been extended to multi-user MIMO systems. Various data-aided and blind CFO estimation techniques have been developed since then [11]–[14]. It has been observed that these algorithms work fine with conventional MIMO systems. However with increase in the number of BS antennas and the number of UTs, these techniques experience prohibitive increase in computational complexity, which makes them unsuited for implementation in massive MIMO systems. Recently in [15] for massive MIMO systems in frequency-flat channels, the authors have proposed an approximation to the joint ML estimator for the CFOs from all UTs. The approximation however requires a multi-dimensional grid search and is therefore expected to have high complexity with large number of UTs.

In this paper we address the problem of *low-complexity* CFO estimation and compensation for a single-carrier massive MU-MIMO BS in a single-cell frequency-selective fading environment. The aim of this paper is mainly twofold: (a) in the first half of the paper, we propose a simple low-complexity CFO estimation algorithm for massive MIMO systems, with special pilot sequences; (b) in the second half of the paper, we analyze the information theoretic performance of a massive MIMO BS uplink (UL) with the proposed CFO estimation and compensation strategy.

For the CFO estimation phase, the contributions presented in this paper are as follows: (i) we propose a simple uplink training scheme that simplifies the CFO estimation and also satisfies the optimality criterion for pilot design with respect to minimizing the CRLB on the variance of the CFO estimation error [9], [11]; (ii) we propose a *low-complexity* multi-user CFO estimation algorithm at the BS and derive a closed-form analytical approximation of the proposed CFO estimate. Exhaustive simulations reveal that the analytically approximate expression for the mean square error (MSE) of the proposed CFO estimation is tight. Also for sufficiently high per-user radiated power the proposed CFO estimator performs close to the CRLB; (iii) analysis of the MSE expression reveals that for a fixed number of UTs, K and a fixed training length N , the required per-user radiated power to achieve a fixed desired MSE can be reduced as $\frac{1}{\sqrt{M}}$, with increasing M , provided that M is sufficiently large (i.e. massive MIMO regime); (iv) in massive MIMO regime, i.e., for fixed and sufficiently large M , fixed pilot length, N , the required per-user radiated power to achieve a fixed desired MSE decreases with increase in K , as long as K is much smaller than the training length; (v) the per-channel use total complexity of the proposed estimator is $\mathcal{O}(M)$ which is independent of the number of users, K . Therefore for a fixed M and fixed $N \gg K$, the number of UTs supported by the BS can be increased without incurring any significant increase in complexity; (vi) for a fixed K and fixed and sufficiently large M , with increasing N it is observed that the required per-user radiated power to achieve a fixed desired MSE decreases as $\frac{1}{\sqrt{N}}$, as long as N is much larger than the number of UTs K . We also observe that for a fixed (M, K) and increasing $N \gg K$, the total required per-user radiated *energy* to maintain a fixed desired MSE first decreases and then begins to increase beyond a critical value of N . Therefore there exists an optimal length of the pilot sequence for the proposed CFO estimator, beyond which increasing N is not energy efficient.

Next we analyze the information theoretic performance of the proposed CFO estimation and compensation strategy in massive MIMO BS uplink (UL). At the beginning CFO estimation is performed in a special UL slot at the BS. These estimates are then fed back to the UTs in the

following downlink (DL) slot. During the UL data transmission, the BS firstly estimates the channel using pilots transmitted by the UTs. These channel estimates are then used for coherent multi-user detection (MUD) of the information symbol transmitted by the UTs. For MUD, we consider the low complexity time-reversal maximal-ratio-combining (TR-MRC) receiver [16]. A major contribution of this paper is the closed-form expression for an achievable information sum-rate of the TR-MRC detector, in the presence of residual CFO estimation error, resulting from the proposed CFO estimation/compensation done prior to data transmission. Our analysis reveals that for a fixed CFO training length N , fixed K and fixed length of UL data transmission block, the required per-user radiated power to achieve a fixed desired information sum-rate decreases by 1.5 dB for every doubling in the number of BS antennas, M (i.e. an $\mathcal{O}(\sqrt{M})$ array gain). This important new result is very interesting since for the ideal no CFO scenario, the best possible array gain is known to be $\mathcal{O}(\sqrt{M})$ (see [8]). This implies that the proposed CFO estimation algorithm does not degrade the achievable array gain of massive MIMO systems in the presence of CFOs. Exhaustive simulations suggest that the proposed CFO estimation/compensation algorithm in fact can achieve sum-rate performance close to that achieved in the no CFO scenario.

Notations: \mathbb{C} denotes the set of complex numbers. \mathbb{E} denotes the expectation operator. $(\cdot)^H$ denotes the complex conjugate transpose operation, while $(\cdot)^*$ denotes the complex conjugate operator. Also, \mathbf{I}_N denotes the $N \times N$ identity matrix.

II. SYSTEM MODEL

We consider a single-carrier multi-user (MU) massive MIMO system, with M base station (BS) antennas, serving K single-antenna autonomous user terminals (UTs) simultaneously in the same time-frequency resource. We also assume that the massive MIMO BS under consideration is operating in a frequency-selective fading environment. Therefore the complex baseband channel model in discrete time is assumed to be a finite impulse response (FIR) filter with L taps. The channel gain between the m^{th} BS antenna and the k^{th} UT at the l^{th} channel tap is given by $h_{km}[l] \triangleq \sigma_{hkl} g_{km}[l]$, ($\sigma_{hkl} > 0$), where $l = 0, 1, \dots, L-1$, $m = 1, 2, \dots, M$ and $k = 1, 2, \dots, K$. Here $g_{km}[l]$ models the fast fading component of the channel gain which we assume to be independent and identically distributed (i.i.d.) and Rayleigh faded, i.e., complex circular symmetric Gaussian with unit variance or $g_{km}[l] \sim \mathcal{CN}(0, 1)$. Note that $\{\sigma_{hkl}^2\}$, $\forall(k, l)$ models the power delay profile (PDP) of the channel. We also assume that the PDP remains fixed for the entire duration of communication and that the BS has perfect knowledge of the PDP. Further

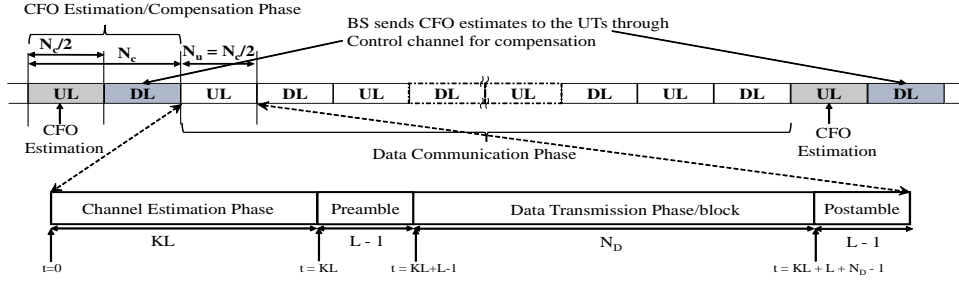


Fig. 1 The communication strategy, depicting allocation of a separate UL/DL TDD slot for CFO estimation and compensation prior to data communication. For UL data communication, the UL slot spans half coherence interval, i.e., $N_u \triangleq \frac{N_c}{2} = KL + N_D + 2(L - 1)$ channel uses. In each UL slot, the first KL channel uses are used for channel estimation at BS using pilot transmission from UTs. The channel estimates acquired in a UL slot are used for downlink beamforming of information to the UTs, in the next DL slot. Note that the length of the DL slot is also $\frac{N_c}{2}$ channel uses.

the channel realization is assumed to remain unchanged over N_c channel uses.¹

A. Communication Strategy

A massive MIMO system is expected to operate in a Time Division Duplexed (TDD) mode. In TDD, each coherence interval is split into an uplink (UL) slot, followed by a downlink (DL) slot. In the UL slot, the UTs transmit pilot signals to the BS for channel estimation, prior to UL data transmission. In the DL, using the same channel estimates, the BS beamforms the information symbols to the UTs.

In a multi-user massive MIMO system, acquisition of the carrier frequency offsets (CFOs) of different UTs at the BS and their compensation is important. Here we propose to first estimate the CFOs at the start of communication, using pilots transmitted by the UTs to the BS in a special UL slot. The BS then feeds these CFO estimates back to the respective users in the following DL slot over a control channel² and the UTs correct their internal oscillators accordingly. From the next UL slot, normal communication starts with the UTs transmitting pilots for channel estimation, followed by UL data transmission. The communication strategy described above is illustrated through Fig. 1. The special UL/DL slots for CFO estimation and compensation might be repeated after every few coherence intervals, depending on how fast the CFO changes.

¹Here N_c is the number of channel uses that span the coherence interval. If T_c is the coherence time in seconds and B_w is the communication bandwidth in Hz, then $N_c = T_c B_w$.

²We consider this feedback to be error-free. However the exact mechanism for this feedback and impact of feedback errors is a topic of future study.

B. Signal Model

Let $a_k[t]$ denote the transmitted signal from the k^{th} UT at time instance t . The signal received at the m^{th} BS antenna from all K UTs at time t is therefore given by³

$$r_m[t] \triangleq \sum_{k=1}^K \sum_{l=0}^{L-1} h_{km}[l] a_k[t-l] e^{j\omega_k t} + n_m[t], \quad (1)$$

where $n_m[t] \sim \mathcal{CN}(0, \sigma^2)$ is the complex circular symmetric additive white Gaussian noise (AWGN). Here $\omega_k \triangleq 2\pi\Delta f_k T_s$, where Δf_k is the offset between the carrier frequency of the received signal from the k^{th} UT and the frequency of the BS oscillator. Also $T_s \triangleq 1/B_w$, where B_w is the communication bandwidth.

III. CFO ESTIMATION

In this section, firstly we present the Cramer-Rao lower Bound (CRLB) for the best possible unbiased CFO estimate (Section III-A). The CRLB also gives us insight into the design of pilot/training sequences, optimal with respect to the minimization of the CRLB for CFO estimation. Various algorithms have been developed for CFO estimation in both single and multi-carrier MIMO systems [10]–[14]. However these existing algorithms incur prohibitive increase in complexity with increasing number of BS antennas and UTs. Therefore these algorithms are not suitable for application in massive MIMO systems. In this regard we propose a simple orthogonal training sequence that satisfies the conditions of optimality for the pilots used for CFO estimation (see Section III-B). Using these pilots, we devise a *low-complexity* technique to estimate the CFO of each user separately (see Section III-C).

A. CRLB for CFO Estimation

Let $(a_k[0], a_k[1], \dots, a_k[N-1])$ be the sequence of pilot symbols transmitted by the k^{th} UT, over $N \leq \frac{N_c}{2}$ channel uses, in the UL slot for CFO estimation (see Fig. 1).⁴ The signal received at the m^{th} BS antenna over the N channel uses is denoted by $\mathbf{r}_m \triangleq (r_m[0], r_m[1], \dots, r_m[N-1])^T$. Using (1), with $t = 0, 1, \dots, N-1$ (here t represents the t^{th} channel use), \mathbf{r}_m is given by [11]

$$\mathbf{r}_m = \sum_{k=1}^K \mathbf{\Gamma}(\omega_k) \mathbf{A}_k \mathbf{h}_{km} + \mathbf{n}_m. \quad (2)$$

Here, $\mathbf{\Gamma}(\omega_k) \triangleq \text{diag}(1, e^{j\omega_k}, e^{j2\omega_k}, \dots, e^{j(N-1)\omega_k})$, $\mathbf{h}_{km} \triangleq (h_{km}[0], h_{km}[1], \dots, h_{km}[L-1])^T$, and $\mathbf{n}_m \triangleq (n_m[0], n_m[1], \dots, n_m[N-1])^T$. Note that $\mathbf{A}_k \in \mathbb{C}^{N \times L}$ is a circulant matrix whose $(t, q)^{\text{th}}$ entry is given by

³In this paper we assume a collocated massive MIMO BS model, i.e. all BS antennas use the same oscillator.

⁴A copy of the last $L-1$ pilot symbols, i.e., $\{a_k[N-L+1], \dots, a_k[N-1]\}$ is transmitted before $\{a_k[0], \dots, a_k[N-1]\}$.

t	Pilot-block $\mathbf{b} = 1$				Pilot-block $\mathbf{b} = 2$				Pilot-block $\mathbf{b} = \mathbf{B} = 3$			
	0	1	2	3	4	5	6	7	8	9	10	11
$a_1[l]$	$\sqrt{KLp_u}$	0	0	0	$\sqrt{KLp_u}$	0	0	0	$\sqrt{KLp_u}$	0	0	0
$a_2[l]$	0	0	$\sqrt{KLp_u}$	0	0	0	$\sqrt{KLp_u}$	0	0	0	$\sqrt{KLp_u}$	0

Fig. 2 Illustration of the Proposed Transmitted Pilot/Training sequence for CFO estimation with $K = 2$, $L = 2$, $N = 12$ (i.e. $B = N/KL = 3$). Here K is the number of UTs, L is the number of channel gain taps, N is the length of the pilot sequence, and B is the number of KL length *pilot-blocks* present in the pilot sequence.

$$A_k(t, q) = \begin{cases} a_k[t - q] & t \geq q \\ a_k[t - q + N] & t < q \end{cases} \quad (3)$$

where $t = 1, 2, \dots, N$, and $q = 1, 2, \dots, L$. The overall received signal vector, $\mathbf{r} \triangleq (\mathbf{r}_1^T, \mathbf{r}_2^T, \dots, \mathbf{r}_M^T)^T$, is thus given by $\mathbf{r} = \mathbf{Q}(\boldsymbol{\omega})\mathbf{h} + \mathbf{n}$, where $\mathbf{h} \triangleq (\mathbf{h}_1^T, \mathbf{h}_2^T, \dots, \mathbf{h}_M^T)^T$ with $\mathbf{h}_m \triangleq (\mathbf{h}_{1m}^T, \mathbf{h}_{2m}^T, \dots, \mathbf{h}_{Km}^T)^T$ [11]. Further, $\mathbf{n} \triangleq (\mathbf{n}_1^T, \mathbf{n}_2^T, \dots, \mathbf{n}_M^T)^T$, and $\boldsymbol{\omega} \triangleq (\omega_1, \omega_2, \dots, \omega_K)^T$.

Also, $\mathbf{Q}(\boldsymbol{\omega}) \triangleq \mathbf{I}_M \otimes [\boldsymbol{\Gamma}(\omega_1)\mathbf{A}_1, \boldsymbol{\Gamma}(\omega_2)\mathbf{A}_2, \dots, \boldsymbol{\Gamma}(\omega_K)\mathbf{A}_K]$. Here ' \otimes ' denotes the Kronecker product for matrices. Based on the above data model, the CRLB for CFO estimation is given by [11]

$$\text{CRLB}(\boldsymbol{\omega}) \triangleq \frac{\sigma^2}{2} \left(\Re \left\{ \mathbf{X}^H \mathbf{P}_Q \mathbf{X} \right\} \right)^{-1}, \quad (4)$$

where $\mathbf{P}_Q \triangleq \mathbf{I}_{MN} - \mathbf{Q}(\boldsymbol{\omega})(\mathbf{Q}^H(\boldsymbol{\omega})\mathbf{Q}(\boldsymbol{\omega}))^{-1}\mathbf{Q}^H(\boldsymbol{\omega})$. The submatrix of \mathbf{X} defined by rows $[(m-1)N+1, \dots, mN]$ in the k^{th} column is given by $\mathbf{X}((m-1)N+1 : mN, k) \triangleq \mathbf{F}\boldsymbol{\Gamma}(\omega_k)\mathbf{A}_k\mathbf{h}_{km} \in \mathbb{C}^{N \times 1}$, where $\mathbf{F} = \text{diag}(0, 1, \dots, N-1)$, $m = 1, 2, \dots, M$, and $k = 1, 2, \dots, K$.

B. Proposed Training Sequence for CFO Estimation

From [9], [11] for large N , the conditions for optimality of the training sequence (i.e. in terms of minimizing the CRLB) is given by

$$\left. \begin{aligned} \mathbf{A}_i^H \mathbf{A}_i &\propto \mathbf{I}_L \\ \mathbf{A}_i^H \mathbf{A}_j &= \mathbf{0}_{L \times L}, \end{aligned} \right\} \forall i \neq j, (i, j) \in \{1, 2, \dots, K\}. \quad (5)$$

In this paper, we propose a set of orthogonal pilot signals which consist of *pilot-blocks*. Each *pilot-block* spans KL channel uses and therefore for a pilot sequence of length N , there are $B \triangleq \frac{N}{KL}$ *pilot-blocks*.⁵ In each *pilot-block*, each of the UTs transmit only a single impulse, preceded and followed by zeros. For instance, in the b^{th} *pilot-block*, the first UT transmits an impulse at $t = (b-1)KL$, the second UT at $t = (b-1)KL + L$, and the K^{th} UT at

⁵We assume N to be an integer multiple of KL .

$t = (b - 1)KL + (K - 1)L$. The impulses from different UTs are separated by L channel uses (which is the maximum delay spread of any user's impulse response). Therefore the signal received at the BS antennas in the time interval $(b - 1)KL + (k - 1)L \leq t \leq (b - 1)KL + (kL - 1)$ will simply be the impulse response of the channel for the k^{th} UT. These KL channel uses (i.e. L channel uses for each of the K users) constitute a *pilot-block* (see Fig. 2). For the k^{th} UT, the overall pilot transmitted over B *pilot-blocks* is given by

$$\mathbf{a}_k[t] = \begin{cases} \sqrt{KLp_u}, & t \bmod KL = (k - 1)L \\ 0, & \text{elsewhere,} \end{cases} \quad (6)$$

where p_u is the average power of the pilot signal transmitted by each UT.⁶

It can be shown that for the pilot/training sequence proposed above in (6), we have $\mathbf{A}_i^H \mathbf{A}_j = \mathbf{0}$ and $\mathbf{A}_i^H \mathbf{A}_i = KLI_L$, when $i \neq j$, $i = 1, 2, \dots, K$ and $j = 1, 2, \dots, K$, i.e., the proposed pilots satisfy the optimality conditions in (5).

C. Proposed CFO Estimate for the k^{th} UT

For the pilot signal proposed in (6), the signal received at the m^{th} BS antenna at time instance $\tau(b, k, l) \triangleq (b - 1)KL + (k - 1)L + l$ is given by $r_m[\tau(b, k, l)] = \sqrt{KLp_u} h_{km}[l] e^{j\omega_k \tau(b, k, l)} + n_m[\tau(b, k, l)]$, where $l = 0, 1, \dots, L - 1$, $k = 1, 2, \dots, K$ and $b = 1, 2, \dots, B$. Since the channel realization remains static over an entire coherence interval, the CFO of a user can be estimated by correlating the impulse responses received from that user in consecutive *pilot-blocks*. The correlation of the received pilots in consecutive blocks, i.e., time instances $\tau(b, k, l)$ and $\tau(b + 1, k, l)$ is given by

$$\begin{aligned} r_m^*[\tau(b, k, l)]r_m[\tau(b + 1, k, l)] &= KLp_u |h_{km}[l]|^2 e^{j\omega_k KL} + \\ &\underbrace{\sqrt{KLp_u} h_{km}^*[l] e^{-j\omega_k \tau(b, k, l)} n_m[\tau(b + 1, k, l)]}_{\triangleq T_1} + \underbrace{\sqrt{KLp_u} h_{km}[l] e^{j\omega_k \tau(b + 1, k, l)} n_m^*[\tau(b, k, l)]}_{\triangleq T_2} + \underbrace{n_m[\tau(b + 1, k, l)] n_m^*[\tau(b, k, l)]}_{\triangleq T_3} \end{aligned} \quad (7)$$

Sum of Noise Terms, $c_k(b, m, l) \triangleq T_1 + T_2 + T_3$.

We observe that the argument of the first term in (7) is $\omega_k KL$, i.e., it depends on the CFO of the k^{th} user, ω_k . Since the argument of this term is independent of the BS antenna index, m , the channel tap l and the *pilot-block* index b , we can average the noise terms in (7) (denoted as $c_k(b, m, l)$) over b , m and l . This averaging is given by

$$\rho_k \triangleq \frac{\sum_{b=1}^{B-1} \sum_{m=1}^M \sum_{l=0}^{L-1} r_m^*[\tau(b, k, l)]r_m[\tau(b + 1, k, l)]}{MKL(B - 1)p_u \sum_{l=0}^{L-1} \sigma_{hkl}^2} = G_k e^{j\omega_k KL} + \nu_k, \quad \text{where} \quad (8)$$

⁶Use of the scaling factor \sqrt{KL} in (6) guarantees that the average power transmitted from each user is p_u , irrespective of the number of users and the number of channel taps.

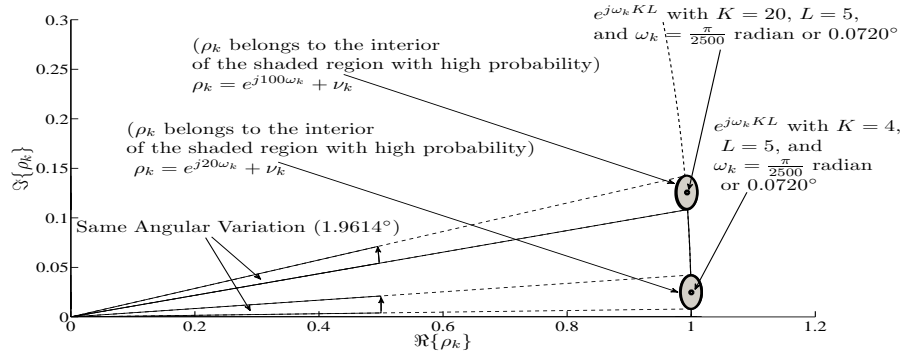


Fig. 3 High probability region of $\rho_k = e^{j\omega_k KL} + \nu_k$ (depicted by the shaded regions in the figure) for $K = 4$ and $K = 20$ (with fixed $L = 5$, $\omega_k = \frac{\pi}{2500}$ radian, or 0.0720° and fixed variance of ν_k). Since the angular variation of the high probability regions of ρ_k for both $K = 4$ and $K = 20$ are the same, the variation in $\hat{\omega}_k = \frac{\arg(\rho_k)}{KL}$ from its true value ω_k is expected to be smaller for a larger K (due to the division of $\arg(\rho_k)$ by K).

$$\nu_k \triangleq \frac{\sum_{b=1}^{B-1} \sum_{m=1}^M \sum_{l=0}^{L-1} c_k(b, m, l)}{MKL(B-1)p_u \sum_{l=0}^{L-1} \sigma_{h_{kl}}^2}, \quad \text{and} \quad G_k \triangleq \left(\frac{\sum_{m=1}^M \sum_{l=0}^{L-1} |h_{km}[l]|^2}{M \sum_{l=0}^{L-1} \sigma_{h_{kl}}^2} \right). \quad (9)$$

From (8) we note that the argument of the first term, $G_k e^{j\omega_k KL}$, depends on the CFO of the k^{th} UT. Also its magnitude, G_k , is independent of the CFO. Therefore, we propose the following estimate of the CFO for the k^{th} user

$$\hat{\omega}_k \triangleq \frac{\arg(\rho_k)}{KL}, \quad (10)$$

where $\arg(c)$ denotes the ‘principal argument’ of the complex number c .

Remark 1. Note that the proposed CFO estimate in (10) is well-defined (i.e. unambiguous) only if $|\omega_k KL| < \pi$. For most practical systems, we believe that this condition will be satisfied.⁷ \square

Remark 2. From (9) and the strong law of large numbers, it follows that for i.i.d. $\{h_{km}[l]\}$, $G_k \rightarrow 1$ as $M \rightarrow \infty$, with probability 1. \square

Remark 3. In the following through Fig. 3, we explain as to why the accuracy of the proposed estimator in (10) is expected to be better for a system having a larger number of UTs. In Fig. 3, the two shaded regions depict the high probability regions of $\rho_k = G_k e^{j\omega_k KL} + \nu_k$ with $G_k = 1$ (see *Remark 2*), for $K = 4$ and $K = 20$ (fixed $L = 5$, $\omega_k = \frac{\pi}{2500}$ radian and fixed variance of ν_k). From the figure, it is clear that with high probability, $\arg(\rho_k) \in (20\omega_k - 0.9807^\circ, 20\omega_k + 0.9807^\circ)$

⁷For instance, with a carrier frequency of $f_c = 2$ GHz, and an oscillator accuracy of 0.1 PPM (parts per million) (commonly used in cellular BSs [18], [19]) the maximum carrier frequency offset is $\Delta f = f_c \times 10^{-7} = 200$ Hz. For a system having a communication bandwidth $B_w = 1$ MHz (i.e., $T_s = 1/B_w = 10^{-6}$ s) this corresponds to a maximum CFO of $\omega_k = 2\pi\Delta f T_s = 2\pi \times 200 \times 10^{-6} = 4\pi \times 10^{-4}$ radian, which is 2500 times less than π . Therefore for massive MIMO systems, even with $K = 10$ and $L = 5$, $|\omega_k KL| = \frac{\pi}{50} \ll \pi$.

when $K = 4$ and $\arg(\rho_k) \in (100\omega_k - 0.9807^\circ, 100\omega_k + 0.9807^\circ)$ when $K = 20$. From (8) and (10) it is clear that the angular variation of these high probability regions depends on the variance of ν_k . With a fixed variance of ν_k , it therefore appears that the angular variation of these high probability regions would remain the same for both $K = 4$ and $K = 20$. Since the proposed estimator is $\hat{\omega}_k = \frac{\arg(\rho_k)}{KL}$, it follows that $\hat{\omega}_k \in (\omega_k - \frac{0.9807^\circ}{KL}, \omega_k + \frac{0.9807^\circ}{KL})$ with high probability. Clearly, this high probability interval shrinks as K increases. Therefore it is expected that the accuracy of the proposed estimator would increase with increasing K .⁸ \square

Remark 4. With a carrier frequency f_c , let the maximum frequency offset for any user be $\Delta f = \kappa f_c$ (note that for mobile terminals, κ might depend on the velocity of the terminal.). Since we must have $|\omega_k KL| < \pi$ and $\omega_k = 2\pi\Delta f T_s$, therefore

$$\pi > |2\pi\Delta f K L T_s| \stackrel{(a)}{=} 2\pi\kappa K f_c T_d, \quad (11)$$

where (a) follows from the fact that $T_d \triangleq L T_s$ is the delay spread of the channel.

Clearly from (11), it follows that, for the proposed CFO estimator in (10) to work, the maximum number of allowed users must be less than $\frac{1}{2\kappa f_c T_d}$. Note that this maximum limit is usually quite large. For example with $f_c = 2$ GHz, $T_d = 5\mu s$ and $\kappa = 0.1$ PPM, we have $K < 500$. \square

Remark 5. From (8) and (10) it is clear that the total number of operations required to compute all the K CFO estimates is $(M(B-1)L+1)K$. Since $N = BKL$, the average number of operations per-channel use is $(M(B-1)L+1)K/N \approx M$ ($N \gg K$). Note that the total per-channel use complexity is independent of K and increases only linearly with M . \square

Lemma 1. The mean and variance of $\nu_k^I \triangleq \Re(\nu_k)$ and $\nu_k^Q \triangleq \Im(\nu_k)$ are given by $\mathbb{E}[\nu_k^I] = \mathbb{E}[\nu_k^Q] = 0$ and

$$\mathbb{E}[(\nu_k^I)^2] = \frac{\frac{G_k}{\gamma_k} \left(1 + \frac{B-2}{B-1} \cos(2\omega_k KL)\right)}{\underbrace{M K L (B-1)}_{(N-KL)}} + \frac{\frac{1}{2K\gamma_k^2}}{\underbrace{M K L (B-1)}_{(N-KL)}}, \quad (12)$$

$$\mathbb{E}[(\nu_k^Q)^2] = \frac{\frac{G_k}{\gamma_k} \left(1 - \frac{B-2}{B-1} \cos(2\omega_k KL)\right)}{M K L (B-1)} + \frac{\frac{1}{2K\gamma_k^2}}{M K L (B-1)}, \quad \text{where } \gamma_k \triangleq \frac{p_u}{\sigma^2} \sum_{l=0}^{L-1} \sigma_{hkl}^2. \quad (13)$$

Proof: See Appendix A. \blacksquare

Remark 6. From (12) and (13) it is clear that $\mathbb{E}[(\nu_k^I)^2]$ and $\mathbb{E}[(\nu_k^Q)^2]$ decrease with increasing number of BS antennas, M . This reduction in the variance of ν_k^I and ν_k^Q with increasing M

⁸From the analytical expressions of the variance of ν_k derived later in (12) and (13), we will see that the above conclusion is indeed true when $N \gg KL$. This is because the variance of ν_k (i.e. variances of ν_k^I and ν_k^Q) does not increase significantly with increasing K as long as $KL \ll N$ (see also *Remark 10* later).

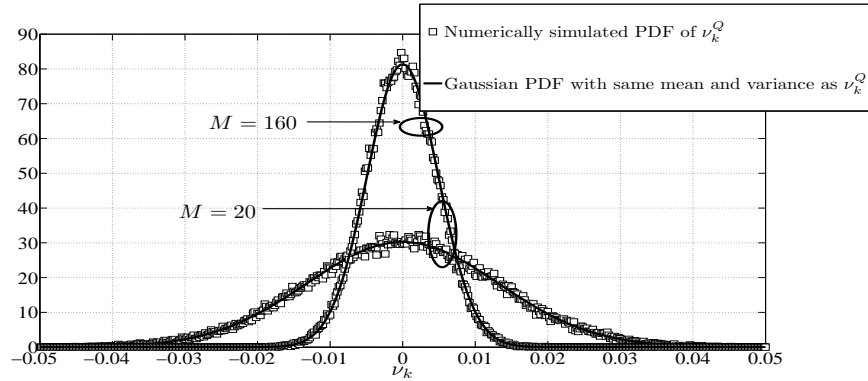


Fig. 4 Numerically computed probability density function (pdf) of ν_k^Q for $M = 20$ (with $G_k \approx 1.0238$) and $M = 160$ (with $G_k \approx 1.0002$) shown by the curves marked with squares (with fixed $K = 10$, $L = 5$, $N = 500$ and $\gamma_k = -10$ dB). Note that for both $M = 20$ and $M = 160$, ν_k^Q is approximately Gaussian distributed (Compare the solid curves with curves marked with squares).

is due to the averaging of the noise terms (defined in (7)) across all M BS antennas (see (9)). Further as $M \rightarrow \infty$, since ν_k^I and ν_k^Q are average of a large number of noise terms (see (9)), it is expected that both ν_k^I and ν_k^Q would be asymptotically Gaussian distributed. This argument is supported through Fig. 4. \square

Theorem 1. (Approximation of the CFO Estimate) If $|\omega_k KL| \ll \pi$ and $\gamma_k \gg \gamma_k^0$, then the proposed CFO estimate in (10) can be approximated by

$$\hat{\omega}_k \approx \omega_k + \frac{\nu_k^Q}{G_k KL}, \text{ where } \gamma_k^0 \triangleq \frac{\frac{B-1}{2B-3}}{KG_k \left[\sqrt{1 + 2ML \frac{(B-1)^3}{(2B-3)^2}} - 1 \right]}. \quad (14)$$

Proof: See Appendix B. \blacksquare

Corollary to Theorem 1: If $|\omega_k KL| \ll \pi$ and $\gamma_k \gg \gamma_k^0$, then the mean square error (MSE) of the proposed CFO estimate for the k^{th} UT is given by

$$\mathbb{E}[(\hat{\omega}_k - \omega_k)^2] \approx \frac{\frac{1}{\gamma_k} \left(\frac{G_k}{B-1} + \frac{1}{2K\gamma_k} \right)}{M(N - KL)(KL)^2 G_k^2}. \quad (15)$$

Proof: For $|\omega_k KL| \ll \pi$ and $\gamma_k \gg \gamma_k^0$, from (14), the expression for CFO estimation error for the k^{th} UT is given by

$$\Delta\omega_k \triangleq \hat{\omega}_k - \omega_k \approx \frac{\nu_k^Q}{G_k KL}. \quad (16)$$

Clearly, $\mathbb{E}[\Delta\omega_k] \approx \frac{\mathbb{E}[\nu_k^Q]}{G_k KL} = 0$ from (16) and also from the fact that ν_k^Q is zero mean (see Lemma 1). The variance of $\Delta\omega_k$, i.e., the mean square error (MSE) is therefore given by

$$\mathbb{E}[(\Delta\omega_k)^2] \approx \frac{\mathbb{E}[(\nu_k^Q)^2]}{G_k^2 (KL)^2}. \quad (17)$$

Further since $|\omega_k KL| \ll \pi$, we have $\cos(2\omega_k KL) \approx 1$. Using (13) in (17) with the approximation $\cos(2\omega_k KL) \approx 1$, we get (15). \blacksquare

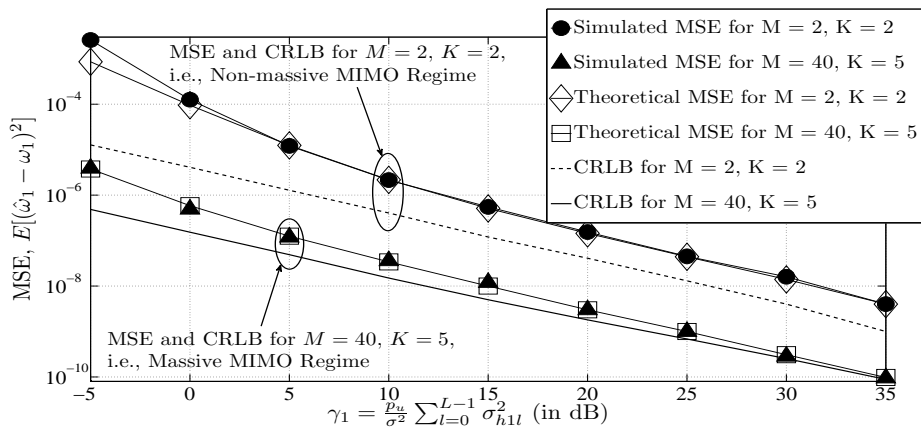


Fig. 5 Plot of Simulated and Theoretical MSE of the proposed CFO estimate for the first UT with varying SNR, compared to the CRLB. Note that the performance gap between the proposed CFO estimate and the CRLB is small in the massive MIMO regime ($M = 40, K = 5$) compared to non-massive MIMO regime ($M = K = 2$). Fixed parameters: $N = 100$ and $L = 2$.

Remark 7. From (15), it is clear that the MSE diminishes with increasing received SNR, γ_k . We also illustrate this through Fig. 5, where we consider the variation in the MSE of the proposed CFO estimate for the first user, i.e., $\mathbb{E}[(\hat{\omega}_1 - \omega_1)^2]$ as a function of increasing SNR, $\gamma_1 = \frac{p_u}{\sigma^2} \sum_{l=0}^{L-1} \sigma_{h_{1l}}^2$. The PDP of the channel is $\sigma_{h_{kl}}^2 = 1/L, l = 0, 1, \dots, L-1$, and $k = 1, 2, \dots, K$. We plot both the theoretical MSE (i.e., expression in the R.H.S. of (15)) and the simulated MSE. Both of these are numerically averaged over channel statistics. We also plot the CRLB (given by (4) and numerically averaged over channel statistics). We have $N = 100$ and $L = 2$. With $M = 40$ and $K = 5$ (i.e. massive MIMO regime), it is observed that the proposed estimator is near optimal at high SNR (i.e. those values of SNR for which $\text{MSE} \ll \omega_k^2$). However with $M = 2$ and $K = 2$ (i.e. non-massive MIMO regime), we note that the proposed estimator does not perform as good as the CRLB. The above observations therefore motivate the use of the proposed estimator for massive MIMO systems. This is even more so because the well-known near-optimal estimators used in conventional small MIMO systems have prohibitive complexity and cannot be used in massive MIMO systems. On the contrary the proposed estimator has *low-complexity* and is therefore well-suited for massive MIMO regime.

Also, for $M = 40$ and $K = 5$, since $G_k \approx 1$ (see *Remark 2*), we have $\gamma_1^0 \approx 0.0055$ (i.e. -22.5 dB, see *Theorem 1*). As can be seen in Fig. 5, for all $\gamma_1 \gg \gamma_1^0 = -22.5$ dB, the simulated MSE (curve marked with triangles) and the theoretical MSE (curve marked with squares) are exactly the same, i.e., the MSE approximation in (15) is tight. Further it can also be shown that if $\gamma_k \gg \gamma_k^0$, then the MSE $\mathbb{E}[(\hat{\omega}_k - \omega_k)^2] \ll \omega_k^2$. \square

Using the **Corollary to Theorem 1**, we present the following propositions.

Proposition 1. If $|\omega_k KL| \ll \pi$, $\gamma_k \gg \gamma_k^0$, and fixed M , K , L and N , the required received SNR, γ_k to achieve a fixed desired MSE $\epsilon > 0$ is approximately given by

$$\gamma_k(\epsilon) \triangleq \frac{G_k/(B-1)}{2\epsilon d} \left[1 + \sqrt{1 + \frac{2(B-1)^2 \epsilon d}{K G_k^2}} \right], \text{ where } d \triangleq M(N-KL)(KL)^2 G_k^2. \quad (18)$$

Proof: Since $|\omega_k KL| \ll \pi$ and $\gamma_k \gg \gamma_k^0$, then from (15), for a desired MSE $\epsilon > 0$, we get

$$\epsilon = \mathbb{E}[(\hat{\omega}_k - \omega_k)^2] = \frac{\frac{1}{\gamma_k} \left(\frac{G_k}{B-1} + \frac{1}{2K\gamma_k} \right)}{M(N-KL)(KL)^2 G_k^2} \implies \epsilon d \gamma_k^2 - \frac{G_k}{B-1} \gamma_k - \frac{1}{2K} = 0, \quad (19)$$

where $d = M(N-KL)(KL)^2 G_k^2$ and $N = BKL$. Solving (19) for the required γ_k , we obtain (18). ■

Remark 8. When $|\omega_k KL| \ll \pi$ and $\gamma_k \gg \gamma_k^0$, then this approximation to the required γ_k is tight, since the approximation of the MSE in (15) is tight (see *Remark 7*). From (18) it follows that for a fixed M , N , K and L , the required $\gamma_k(\epsilon)$ increases with decreasing desired MSE, ϵ . □

Proposition 2. (*Impact of the Number of BS Antennas*) Consider $|\omega_k KL| \ll \pi$ and $\gamma_k \gg \gamma_k^0$. For M sufficiently large, i.e.,

$$M \gg \frac{K}{2\epsilon(N-KL)^3}, \quad (20)$$

and fixed K , L , and N , the required SNR to achieve a fixed desired MSE $\epsilon > 0$ is inversely proportional to \sqrt{M} , i.e., $\gamma_k(\epsilon) \propto 1/\sqrt{M}$.

Proof: From (20), we have

$$2\epsilon(N-KL)^3 M \gg K \implies \frac{2(B-1)^2 \epsilon d}{K G_k^2} \gg 1 \quad (21)$$

where $d = M(N-KL)(KL)^2 G_k^2$ and $N = BKL$. From (21) it follows that

$$\left[1 + \sqrt{1 + \frac{2(B-1)^2 \epsilon d}{K G_k^2}} \right] \approx \sqrt{\frac{2(B-1)^2 \epsilon d}{K G_k^2}}. \quad (22)$$

Using the approximation from (22) in (18), we get

$$\gamma_k(\epsilon) \approx \frac{G_k}{2\epsilon d} \sqrt{\frac{2\epsilon d}{K G_k^2}} \stackrel{(a)}{=} \frac{1/\sqrt{M}}{\sqrt{\epsilon K^3 L^2 (N-KL) G_k^2}}, \quad (23)$$

where (a) follows from $d = M(N-KL)(KL)^2 G_k^2$. It is clear from (23) that with fixed K , L and N , for a desired MSE, ϵ , $\gamma_k(\epsilon)$ decreases as $1/\sqrt{M}$ with increasing M . ■

Remark 9. From Proposition 2 it follows that for a fixed N , K , L and a fixed desired MSE ϵ , the required received SNR $\gamma_k(\epsilon)$ decreases approximately by 1.5 dB with every doubling in the number of BS antennas. This is illustrated through Fig. 6a for the following fixed parameters: $\epsilon = 10^{-8} \ll \omega_1^2$ ($\omega_1 = \pi/2500$), $K = 10$, $L = 5$. Here $T_c = 1$ ms is the coherence interval and $B_w = 1$ MHz is the communication bandwidth. Therefore $N_c = T_c B_w = 1000$ and $N = N_c/2 =$

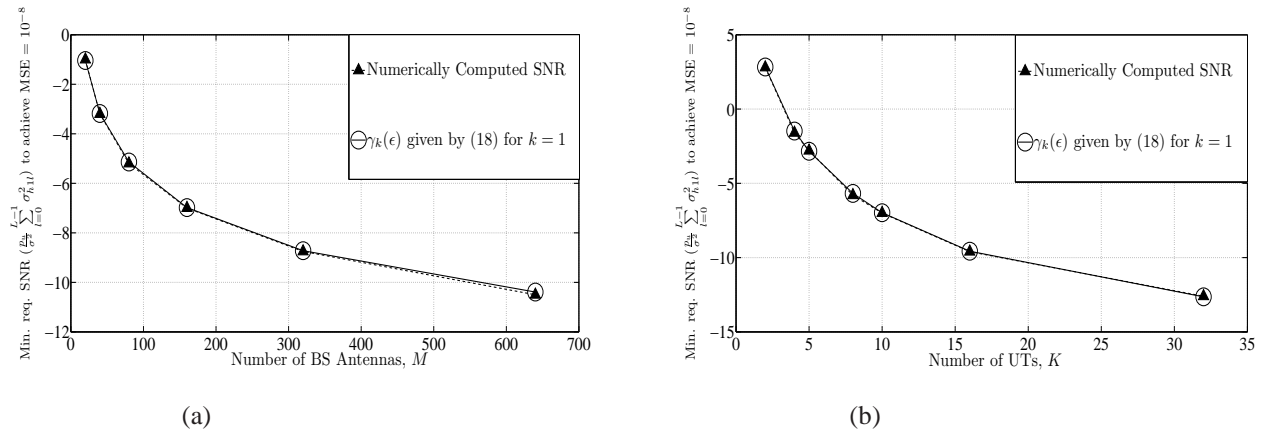


Fig. 6 Plot of the required SNR to achieve a fixed desired MSE, $\epsilon = \mathbb{E}[(\hat{\omega}_1 - \omega_1)^2] = 10^{-8}$ with (a) increasing number of BS antennas, M for fixed $K = 10$; and (b) increasing number of UTs, K for fixed $M = 160$. Fixed parameters: $N = 500$, $L = 5$, $\omega_1 = \frac{\pi}{2500}$.

500. In Fig. 6a we plot both the analytical expression for the required SNR (from (18)) and also the numerically computed exact value of the required SNR. As can be seen from the figure, the analytical approximation to the exact required SNR is indeed tight. From the plotted curves in the figure it is clear that the required SNR decreases by roughly 1.5 dB with every doubling in M . This supports Proposition 2. We explain this observation in the following. For a fixed N , K and L and a fixed desired MSE, ϵ , the variance of ν_k^Q must also be fixed (see (17)). In (17) note that for sufficiently large M , $G_k \approx 1$ with high probability. The variance of ν_k^Q is therefore given by the R.H.S. of (13) which consists of two terms, the first term is proportional to $1/M\gamma_k$ and the second term is proportional to $1/M\gamma_k^2$. Therefore, for a fixed variance of ν_k^Q , γ_k cannot be reduced faster than $1/\sqrt{M}$ with increasing M , since otherwise the second term will increase with increasing M . \square

Remark 10. When $KL \ll N$ and M is sufficiently large (see (20)), the required SNR $\gamma_k(\epsilon)$ to achieve a desired MSE ϵ is approximately given by (replacing $(N - KL)$ by N in (23))

$$\gamma_k(\epsilon) \approx \frac{1}{K^{3/2}} \frac{1}{\sqrt{2\epsilon M N L^2 G_k^2}}. \quad (24)$$

From (24) it is clear that with fixed M , L , N , fixed desired MSE ϵ and with increasing K , the required SNR $\gamma_k(\epsilon)$ decreases with increasing K as long as $KL \ll N$. This is depicted through Fig. 6b, where we plot the required SNR $\frac{p_0}{\sigma^2} \sum_{l=0}^{L-1} \sigma_{hkl}^2$ for $k = 1$ (both the analytical expression in (18) with $G_k = 1$ and the numerically computed SNR) as a function of increasing number of UTs, K for fixed $\epsilon = 10^{-8} \ll \omega_1^2$ ($\omega_1 = \frac{\pi}{2500}$) and $M = 160$, $L = 5$, $N = N_c/2 = 500$ ($N_c = T_c B_w$, $T_c = 1$ ms and $B_w = 1$ MHz.). From Fig. 6b it is also observed that the approximation in (18) is tight.

In the following we explain why the MSE decreases with increasing K (fixed M , L and N). From (10) we note that the estimate $\hat{\omega}_k$ is $1/KL$ times $\arg(\rho_k)$. The division by K helps in reducing the impact of the noise term in ρ_k (i.e. ν_k , see (8) and (9)) on the MSE of the proposed estimate. Note that the division of $\arg(\rho_k)$ by KL is only because the proposed *pilot-blocks* are spaced KL channel uses apart.⁹ Further the variance of the noise term in ρ_k (i.e. ν_k) is also a function of K (see (12) and (13)). In both (12) and (13), both the terms on the R.H.S. have $MKL(B-1) = M(N-KL)$ in the denominator. For $KL \ll N$, $(N-KL) \approx N$ and therefore the first term on the R.H.S. of both (12) and (13) does not vary significantly with increasing K .¹⁰ However the second term on the R.H.S. has $1/2K\gamma_k^2$ in the numerator and therefore for a fixed γ_k it decreases with increasing K .¹¹ Therefore for a fixed γ_k , the variance of the noise term in ρ_k also decreases with increasing K as long as $KL \ll N$. Hence for a fixed γ_k , the division of $\arg(\rho_k)$ by K and the reduction in the variance of ν_k with increasing K , results in reduction of the MSE of $\hat{\omega}_k$ with increasing K . This automatically implies that for a desired MSE ϵ the required SNR $\gamma_k(\epsilon)$ decreases with increasing K (see Fig. 6b).

In *Remark 5* we have seen that the total per-channel use complexity of the proposed CFO estimator does not increase with increasing K ($N \gg K$). Therefore, with increasing K ($N \gg KL$), the required SNR $\gamma_k(\epsilon)$ to achieve a fixed MSE ϵ decreases with no increase in complexity, which is interesting. \square

Proposition 3. (*Impact of the Training Length*) Consider $|\omega_k KL| \ll \pi$ and $\gamma_k \gg \gamma_k^0$. For N sufficiently large, i.e.,

$$N \gg KL + \left(\frac{K}{2\epsilon M} \right)^{1/3}, \quad (25)$$

and fixed K , L , and M , the required SNR $\gamma_k(\epsilon)$ to achieve a fixed desired MSE $\epsilon > 0$ decreases with increasing N .

Proof: From (25), we have $(N-KL)^3 \gg \frac{K}{2\epsilon M} \implies \frac{2(B-1)^2 \epsilon d}{K G_k^2} \gg 1$, where $N = BKL$ and $d = M(N-KL)(KL)^2 G_k^2$. With the condition derived above and using steps similar to (21)-(23), we get

$$\gamma_k(\epsilon) \approx \frac{1}{\sqrt{(N-KL)}} \frac{1}{\sqrt{2\epsilon M K^3 L^2 G_k^2}}. \quad (26)$$

Clearly from (26), with fixed M , K , L and a fixed desired MSE ϵ , $\gamma_k(\epsilon)$ decreases with increasing N . \blacksquare

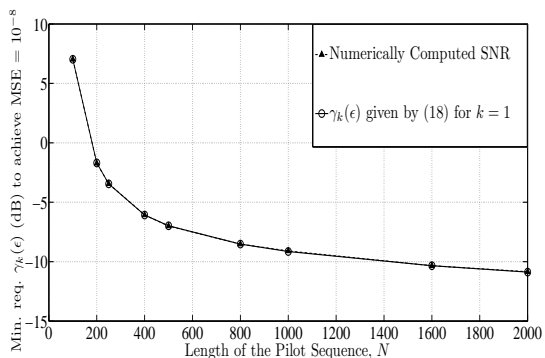
⁹In (7), the correlation $r_m^*[\tau(b, k, l)]r_m[\tau(b+1, k, l)]$ between adjacent *pilot-blocks* leads to the term $KL p_u |h_{km}[l]|^2 e^{j\omega_k KL}$.

¹⁰Here we also use the fact that $\cos(2\omega_k KL) \approx 1$, since $|\omega_k KL| \ll \pi$.

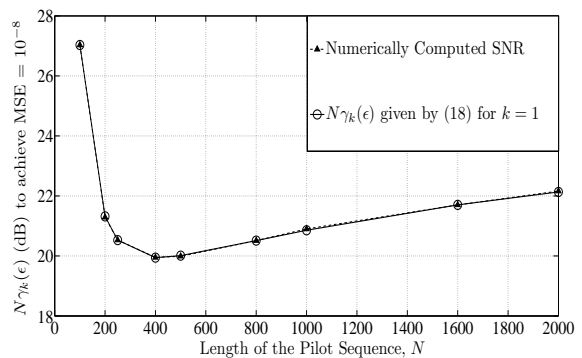
¹¹Note that the second term in the R.H.S. of (12) and (13) is proportional to $1/K$ due to the fact that the pilot used is an impulse which is transmitted once every KL channel uses and therefore its instantaneous power is KL times higher than the average transmitted power, p_u (see (6)).

Remark 11. From Proposition 3 it is observed that when $KL \ll N$, $\gamma_k(\epsilon) \propto 1/\sqrt{N}$ (replacing $(N - KL)$ with N in (26)), i.e., the required SNR decreases by approximately 1.5 dB with every doubling in N (length of the pilot sequence). We illustrate this observation through Fig. 7a where we plot the required SNR $\gamma_k(\epsilon)$ as a function of increasing N for a fixed $M = 160$, $K = 10$, $L = 5$ and MSE $\epsilon = 10^{-8} \ll \omega_1^2$ ($\omega_1 = \pi/2500$). It can be seen that for a fixed MSE, the required SNR $\gamma_k(\epsilon)$ decreases by almost 1.5 dB when N increases from $N = 1000$ to $N = 2000$ (note that $N = 1000 \gg KL = 50$). We explain the above observation in the following. Since every user transmits a single impulse every KL channel uses and $N = BKL$, with increasing N , we have more pilot blocks (i.e. larger B) which results in better averaging of the noise term in (7) (see also (9)). From the R.H.S. of (13), the variance of ν_k^Q consists of two terms, the first term is proportional to $\frac{1}{(N-KL)\gamma_k}$ and the second term is proportional to $\frac{1}{(N-KL)\gamma_k^2}$. Clearly for a fixed desired MSE ϵ , and therefore fixed variance of ν_k^Q (evident from (17)) the required $\gamma_k(\epsilon)$ cannot decrease at a rate more than $\sqrt{(N - KL)} \approx \sqrt{N}$ (as long as $KL \ll N$), since otherwise the second term would increase with N .

The total per-user radiated energy for CFO estimation is $NT_s p_u$ Joule and the received per-user energy is $NT_s p_u \sum_{l=0}^{L-1} \sigma_{h_{kl}}^2$ Joule. Note that since noise variance $\sigma^2 = N_0 B_w$ (N_0 is the power spectral density (PSD) of the AWGN and $B_w = 1/T_s$ is the communication bandwidth), the ratio of the received total per-user energy to the noise PSD is given by $\frac{NT_s p_u}{N_0} \sum_{l=0}^{L-1} \sigma_{h_{kl}}^2 = N \frac{p_u}{\sigma^2} \sum_{l=0}^{L-1} \sigma_{h_{kl}}^2 = N\gamma_k$. In Fig. 7b we plot $N\gamma_k(\epsilon)$ as a function of increasing N for the same set of fixed parameters as in Fig. 7a (i.e. $M = 160$, $K = 10$, $L = 5$, and MSE $\epsilon = 10^{-8}$). It is



(a)



(b)

Fig. 7 Plot of the required SNR to achieve a fixed desired MSE, $\epsilon = 10^{-8}$ with increasing pilot sequence length, N , for the following fixed parameters: $M = 160$, $K = 10$, $L = 5$ (see Figure (a) on the left). Also variation of the ratio of the total received per-user energy to noise PSD, i.e., $N\gamma_k(\epsilon)$ with increasing training length N is plotted (see Figure (b) on the right) for the same fixed parameters ($M = 160$, $K = 10$, $L = 5$).

observed that when $N \gg KL$ (i.e., $N > 10KL$ in the figure), the required ratio of the received total per-user pilot energy to noise PSD (i.e. $N\gamma_k(\epsilon)$) increases as \sqrt{N} , with increasing N . Also we observe that for relatively small N , $N\gamma_k(\epsilon)$ first decreases with increasing N and when N becomes significantly larger than KL , it starts to increase with increasing N . There is therefore an optimal $N = N^*$ which minimizes the total radiated per-user pilot energy for CFO estimation (see Fig. 7b). Hence even if the maximum allowed length of the pilot sequence is greater than N^* , i.e., $N_c/2 > N^*$, it makes sense to have a pilot sequence of length no more than $N = N^*$, so as to minimize the radiated total per-user pilot energy. \square

IV. UPLINK DATA COMMUNICATION

After the CFO estimation and compensation phase, we have the data communication phase (see Fig. 1). Each coherence interval in the data communication phase is split into an UL slot and a DL slot. As shown in Fig. 1, in the UL slot, the UTs transmit pilot signals for channel estimation at the BS (KL channel uses). It is then followed by a preamble sequence of $L - 1$ channel uses and subsequently by the data communication phase of N_D channel uses. In the data communication phase, the BS performs coherent multi-user detection, using the CSI acquired in the channel estimation phase. The data transmission phase/block is then followed by a post-amble sequence of $L - 1$ channel uses.

A. Channel Estimation

Here we propose a simple UL pilot sequence of length KL channel uses for channel estimation. The pilot sequence for the k^{th} user, i.e., $s_k[t]$, ($0 \leq t \leq KL - 1$) is given by

$$s_k[t] = \begin{cases} \sqrt{KLp_u}, & t = (k-1)L \\ 0, & \text{otherwise,} \end{cases} \quad (27)$$

i.e., the k^{th} UT only transmits an impulse at the $\{(k-1)L\}^{\text{th}}$ channel use. This simple pilot sequence design allows for a simple channel estimation scheme, since the impulses are temporally separated by more than $(L-1)$ channel uses and therefore their impulse responses do not overlap in time. The received pilot from the k^{th} UT at the m^{th} BS antenna at time $t = (k-1)L + l$ is given by

$$r_m[(k-1)L + l] = \sqrt{KLp_u}h_{km}[l]e^{j\Delta\omega_k((k-1)L+l)} + n_m[(k-1)L + l], \quad (28)$$

where $l = 0, 1, \dots, L - 1$ and $\Delta\omega_k = \hat{\omega}_k - \omega_k$ is the residual CFO after compensation ($\hat{\omega}_k$ is the proposed CFO estimate in (10)). Here $n_m[(k-1)L + l] \sim \mathcal{CN}(0, \sigma^2)$ is i.i.d. circular symmetric AWGN noise. Note that $h_{km}[l]$ appears in $r_m[t]$ only for $t = (k-1)L + l$ since the

k^{th} UT's pilot signal is an impulse at $t = (k-1)L$. Therefore $h_{km}[l]$ can only be estimated from $r_m[(k-1)L+l]$. The maximum likelihood (ML) estimate of $h_{km}[l]$ using $r_m[(k-1)L+l]$ from (28) is given by

$$\hat{h}_{km}[l] \triangleq \frac{1}{\sqrt{KLp_u}} r_m[(k-1)L+l] = h_{km}[l] \overbrace{e^{j\Delta\omega_k((k-1)L+l)}}^{\text{Phase Error}} + \overbrace{\frac{n_m[(k-1)L+l]}{\sqrt{KLp_u}}}_{\text{AWGN Noise}}. \quad (29)$$

Note that the channel estimates are distorted by (a) the circular symmetric AWGN noise, and (b) the phase error accumulated over time due to the residual CFO.

B. Maximal Ratio Combining with Time Reversal (TR-MRC) Processing

From Fig. 1, it is clear that the uplink data transmission phase/block starts at $t = (KL+L-1)^{\text{th}}$ channel use and continues for the next $N_D - 1$ channel uses. Let $\sqrt{p_u}x_k[t]$ be the information symbol transmitted by the k^{th} UT at the t^{th} channel use. The signal received at the m^{th} BS antenna in the t^{th} channel use is given by

$$r_m[t] \triangleq \sqrt{p_u} \sum_{k=1}^K \sum_{l=0}^{L-1} h_{km}[l] e^{j\Delta\omega_k t} x_k[t-l] + n_m[t], \quad (KL+L-1) \leq t \leq (KL+L+N_D-2). \quad (30)$$

Here $n_m[t]$ are i.i.d. complex circular symmetric AWGN noise variables with variance σ^2 . In this paper, we consider $x_k[t]$ to be i.i.d. complex circular symmetric Gaussian with unit variance, i.e., $x_k[t] \sim \mathcal{CN}(0, 1)$. In (30), p_u is the average power radiated by each UT in the uplink.

Low-complexity time-reversal maximal ratio combining (TR-MRC) has been shown to achieve near-optimal multi-user detection (MUD) performance in frequency-selective channels without CFO [16].¹² Therefore [16] does not analyze the impact of the residual CFO on the achievable information sum-rate in the uplink. For the k^{th} UT, the output of the TR-MRC detector at time t is given by

$$\hat{x}_k[t] \triangleq \sum_{m=1}^M \sum_{l=0}^{L-1} r_m[t+l] \hat{h}_{km}^*[l], \quad (KL+L-1) \leq t \leq (KL+L+N_D-2). \quad (31)$$

where $\hat{h}_{km}[l]$ is the proposed channel estimate in (29).

V. PERFORMANCE METRIC: ACHIEVABLE SUM-RATE

To assess the performance of the proposed uplink massive MIMO system with CFO estimation and compensation, we derive an achievable information sum-rate. We then quantify the impact of CFO estimation error on the achievable information sum-rate. Using the expression of $\hat{h}_{km}[l]$ from (29) and the expression of $r_m[t]$ from (30) in (31), the output of the TR-MRC detector can be expressed as

¹²Note that [16] only considers modelling of phase noise at the oscillators of the BS and the UTs. The modelling of CFO is however not considered.

$$\begin{aligned}
\hat{x}_k[t] &= \sum_{m=1}^M \sum_{l=0}^{L-1} \left(\overbrace{\sqrt{p_u} \sum_{q=1}^K \sum_{l'=0}^{L-1} h_{qm}[l'] e^{j\Delta\omega_q(t+l)} x_q[t-l'+l] + n_m[t+l]}^{r_m[t+l]} \right) \left(\overbrace{h_{km}^*[l] e^{-j\Delta\omega_k((k-1)L+l)} + \frac{n_m^*[(k-1)L+l]}{\sqrt{KLp_u}}}_{\hat{h}_{km}^*[l]} \right) \\
&= \left(\underbrace{\sqrt{p_u} \sum_{m=1}^M \sum_{l=0}^{L-1} |h_{km}[l]|^2 e^{j\Delta\omega_k(t-(k-1)L)} x_k[t]}_{\triangleq A_k[t]} \right) + \text{ISI}_k[t] + \text{MUI}_k[t] + \text{EN}_k[t], \quad (32)
\end{aligned}$$

where $(KL + L - 1) \leq t \leq (KL + L + N_D - 2)$. Here $A_k[t]$ is the scaling factor of the desired signal component, $A_k[t]x_k[t]$. Further in (32) the inter-symbol interference term (i.e. $\text{ISI}_k[t]$) and the multi-user interference term (i.e. $\text{MUI}_k[t]$) for $(KL + L - 1) \leq t \leq (KL + L + N_D - 2)$ are given by

$$\text{ISI}_k[t] \triangleq \sqrt{p_u} \sum_{m=1}^M \sum_{l=0}^{L-1} \sum_{\substack{l'=0, \\ l' \neq l}}^{L-1} h_{km}[l'] h_{km}^*[l] e^{j\Delta\omega_k(t-(k-1)L)} x_k[t-l'+l], \quad \text{and} \quad (33)$$

$$\text{MUI}_k[t] \triangleq \sqrt{p_u} \sum_{m=1}^M \sum_{l=0}^{L-1} \sum_{\substack{q=1, \\ q \neq k}}^K \sum_{l'=0}^{L-1} h_{qm}[l'] h_{km}^*[l] x_q[t-l'+l] e^{j(\Delta\omega_q(t+l) - \Delta\omega_k((k-1)L+l))}. \quad (34)$$

Also in (32) the effective noise term (i.e. $\text{EN}_k[t]$) is given by

$$\begin{aligned}
\text{EN}_k[t] &\triangleq \underbrace{\sqrt{\frac{1}{KL}} \sum_{m=1}^M \sum_{l=0}^{L-1} \sum_{q=1}^K \sum_{l'=0}^{L-1} h_{qm}[l'] x_q[t-l'+l] n_m^*[(k-1)L+l] e^{j\Delta\omega_q(t+l)}}_{\triangleq N_{1k}[t]} + \\
&\quad \underbrace{\sum_{m=1}^M \sum_{l=0}^{L-1} n_m[t+l] h_{km}^*[l] e^{-j\Delta\omega_k((k-1)L+l)}}_{\triangleq N_{2k}[t]} + \underbrace{\frac{1}{\sqrt{KLp_u}} \sum_{m=1}^M \sum_{l=0}^{L-1} n_m[t+l] n_m^*[(k-1)L+l]}_{\triangleq N_{3k}[t]} \quad (35)
\end{aligned}$$

A. Coding Strategy

From (32) we have

$$\hat{x}_k[t] = \underbrace{\mathbb{E}[A_k[t]] x_k[t]}_{\triangleq \text{ES}_k[t]} + \underbrace{\left(A_k[t] - \mathbb{E}[A_k[t]] \right) x_k[t]}_{\triangleq \text{SIF}_k[t], \text{ Self Interfering component of the signal}} + \underbrace{\text{ISI}_k[t] + \text{MUI}_k[t] + \text{EN}_k[t]}_{\triangleq W_k[t], \text{ Overall effective Noise}} \quad (36)$$

where $\mathbb{E}[A_k[t]]$ is the mean value of $A_k[t]$ across several uplink data transmission blocks (i.e. several channel realizations) and is a function of t . The same is true about the variance of the overall effective noise, $W_k[t]$ in (36). Further for a given t , across multiple uplink data transmission blocks, the realizations of $W_k[t]$ are i.i.d. Hence for a given t , we have an additive noise SISO (single-input single-output) channel in (36) when viewed across multiple uplink data transmission blocks. Therefore for each user there are N_D different SISO channels having distinct

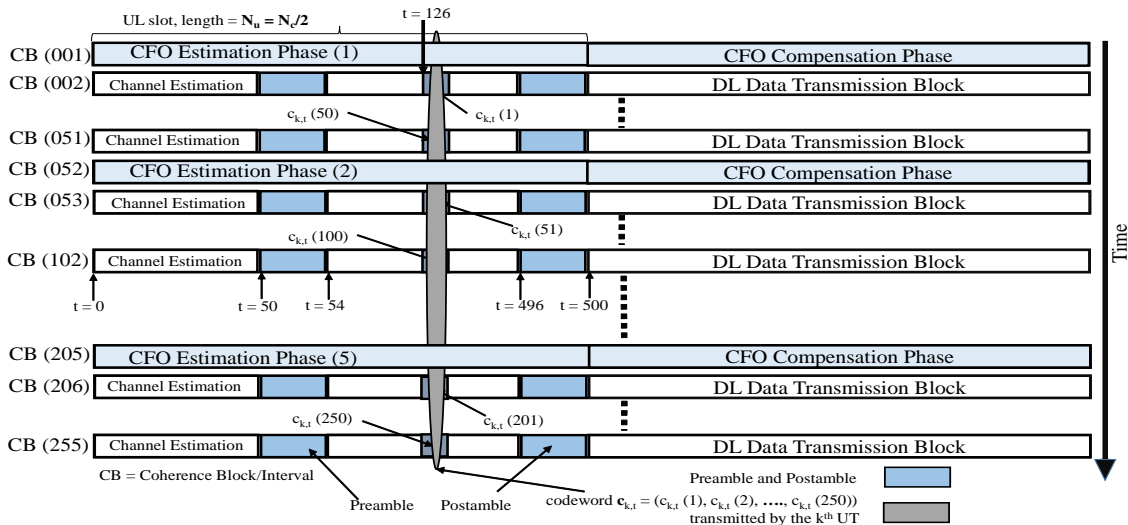


Fig. 8 Proposed coding strategy for uplink data communication, with channel codes spread across multiple channel realizations and also across multiple CFO estimation/compensation phases (in the depicted example, across 5 CFO estimation/compensation phases). In the example shown above, a codeword $c_{k,t} = (c_{k,t}(1), c_{k,t}(2), \dots, c_{k,t}(250))$ from the k^{th} UT for the t^{th} channel use spans 255 coherence intervals/blocks (including CFO estimation/compensation phases). During detection at the BS, all these 250 codeword symbols received at the t^{th} channel use are jointly decoded. Here in the example $K = 10$, $L = 5$, $N_u = N_c/2 = 500$, where N_u is the length of the UL slot.

channel statistics. This leads us to consider N_D channel codes for each user, one for each of the N_D channel uses in the uplink data transmission block, i.e., the k^{th} UT transmits the symbols for its t^{th} channel code ($t = KL+L-1, KL+L, \dots, KL+L+N_D-2$) only during the t^{th} channel use of each uplink data transmission block. We illustrate this through Fig. 8. In Fig. 8, we show 255 different coherence intervals across which one codeword is communicated. The first coherence interval is used for CFO estimation/compensation. This is then followed by 50 UL/DL data transmission phases/blocks. This pattern of one CFO estimation/compensation block, followed by 50 UL/DL transmission blocks is repeated 5 times. Hence the total number of coherence intervals used for communicating a codeword is 255. Let $c_{k,t} \triangleq (c_{k,t}(1), c_{k,t}(2), \dots, c_{k,t}(250))$ denote a codeword from the t^{th} channel code for the k^{th} UT. Here $c_{k,t}(u)$ is the u^{th} symbol of the codeword $c_{k,t}$. In the proposed coding scheme, the coded symbol $c_{k,t}(1)$ is transmitted by the k^{th} UT at the t^{th} channel use of the second coherence block. Similarly $c_{k,t}(50)$ and $c_{k,t}(250)$ are transmitted by the k^{th} UT at the t^{th} channel use of the 51st and the 255th coherence blocks respectively.

Similarly at the BS, for the k^{th} UT, the post TR-MRC symbols in the t^{th} channel use (i.e., $\hat{x}_k[t]$) across different uplink data transmission phases/blocks are jointly decoded. In essence, at the BS, we have N_D parallel channel decoders for each user. The above scheme of N_D parallel

channel codes is however proposed only to derive an achievable lower bound on the information sum-rate. In practice however channel coding/decoding would not be performed across a huge number of uplink data transmission blocks in order to reduce complexity and latency. Instead, coding could be performed across a group of consecutive channel uses within each transmission block (since the statistics of $W_k[t]$ and $A_k[t]$ will not change significantly within a small group of consecutive channel uses).

B. Achievable Information Rate

In the following we derive an achievable information rate for the proposed coding strategy described in Section V-A. Firstly in (36) we note that the correlation between the desired signal term $\text{ES}_k[t]$ and the overall effective noise term $W_k[t]$ is zero, i.e.,

$$\begin{aligned}
\mathbb{E} [\text{ES}_k[t] W_k^*[t]] &= \mathbb{E} \left[\mathbb{E} [A_k[t]] x_k[t] \left\{ \text{SIF}_k[t] + \text{ISI}_k[t] + \text{MUI}_k[t] + \text{EN}_k[t] \right\}^* \right] \\
&= \mathbb{E} [A_k[t]] \left[\underbrace{\mathbb{E} [x_k[t] \text{SIF}_k^*[t]]}_{= 0, \text{ since all } x_k[t] \text{ are i.i.d.}} + \underbrace{\mathbb{E} [x_k[t] \left\{ \text{ISI}_k[t] + \text{MUI}_k[t] \right\}^*]}_{= 0 \text{ (since all } n_m[t] \text{ are i.i.d., zero mean and independent of } x_k[t])} + \underbrace{\mathbb{E} [x_k[t] \text{EN}_k^*[t]]}_{= 0} \right] \\
&= \mathbb{E} [A_k[t]] \left[\underbrace{\mathbb{E} [x_k[t] \left\{ A_k[t] x_k[t] - \mathbb{E} [A_k[t]] x_k[t] \right\}^*]}_{= 0, \text{ since } x_k[t] \text{ and } A_k[t] \text{ are independent}} \right] = 0. \tag{37}
\end{aligned}$$

Since the information symbols $x_k[t]$ in (36) are Gaussian distributed, a lower bound on the information rate for the effective channel in (36) is given by considering the worst case uncorrelated additive noise (in terms of mutual information). With Gaussian information symbols, the worst case uncorrelated noise is Gaussian, with the same variance as $W_k[t]$ [20]. Consequently we obtain a lower bound on the mutual information as follows

$$I(\hat{x}_k[t]; x_k[t]) \geq \log_2 (1 + \text{SINR}_k[t]), \quad \text{where } \text{SINR}_k[t] \triangleq \frac{\mathbb{E} [|\text{ES}_k[t]|^2]}{\mathbb{E} [|W_k[t]|^2]} = \frac{|\mathbb{E} [A_k[t]|^2]}{\mathbb{E} [|W_k[t]|^2]}, \quad \text{and} \tag{38}$$

$$\mathbb{E} [A_k[t]] \stackrel{(a)}{=} \mathbb{E} \left[\sqrt{p_u} \sum_{m=1}^M \sum_{l=0}^{L-1} |h_{km}[l]|^2 \right] \mathbb{E} [e^{j\Delta\omega_k(t-(k-1)L)}] \stackrel{(b)}{=} \sqrt{p_u} M \left(\sum_{l=0}^{L-1} \sigma_{hkl}^2 \right) e^{-\sigma_{\omega_k}^2 (t-(k-1)L)^2/2}. \tag{39}$$

Here step (a) follows from the fact that $\Delta\omega_k$ and $h_{km}[l]$, $l = 0, 1, \dots, L-1$, are independent because CFO estimation and data transmission happen in different coherence intervals. Step (b) follows from the fact that $\Delta\omega_k$ is approximately Gaussian distributed for large M . This is supported by the fact that $\Delta\omega_k = \hat{\omega}_k - \omega_k \approx \frac{\nu_k^Q}{G_k KL}$ (see (16)), and ν_k^Q tends to be Gaussian distributed with increasing M (see Fig. 4 and Remark 6). Using (39), the expression of $\mathbb{E} [|\text{ES}_k[t]|^2]$ is given in Table I.¹³

¹³In Table I, $\sigma_{\omega_k}^2 = \mathbb{E}[(\hat{\omega}_k - \omega_k)^2]$ where $\hat{\omega}_k$ is the proposed CFO estimate defined in (10) and the expectation is taken across multiple CFO estimation phases.

Similarly from (33) and (34) we observe that $\mathbb{E}[\text{ISI}_k[t]] = \mathbb{E}[\text{MUI}_k[t]] = 0$ since $h_{km}[l]$ and $x_k[t]$ are all zero mean and independent. Also $\mathbb{E}[\text{SIF}_k[t]] = 0$ (see (36)). The variance of these terms, i.e., $\text{ISI}_k[t]$, $\text{MUI}_k[t]$ and $\text{SIF}_k[t]$ are also listed in Table I. Further since $n_m[t]$, $h_{km}[l]$ and $x_k[t]$ are zero mean and independent, we have $\mathbb{E}[N_{ik}[t]] = 0$, $\forall i = 1, 2, 3$ ($N_{ik}[t]$ are defined in (35)). Therefore $\mathbb{E}[\text{EN}_k[t]] = \mathbb{E}[N_{1k}[t] + N_{2k}[t] + N_{3k}[t]] = 0$. Also, $\mathbb{E}[N_{1k}[t]N_{2k}^*[t]] = 0$, i.e., $N_{1k}[t]$ and $N_{2k}[t]$ are uncorrelated. Similarly, $\mathbb{E}[N_{2k}[t]N_{3k}^*[t]] = \mathbb{E}[N_{3k}[t]N_{1k}^*[t]] = 0$. Hence the variance of $\text{EN}_k[t]$ is given by $\mathbb{E}[|\text{EN}_k[t]|^2] = \mathbb{E}[|N_{1k}[t]|^2] + \mathbb{E}[|N_{2k}[t]|^2] + \mathbb{E}[|N_{3k}[t]|^2]$ and its expression is listed in Table I.

TABLE I LIST OF VARIANCE OF ALL COMPONENTS OF $W_k[t]$ AND OF THE EFFECTIVE DESIRED SIGNAL $\text{ES}_k[t]$.

Signal/Noise Component	Variance
$\text{ES}_k[t]$	$\mathbb{E}[\text{ES}_k[t] ^2] = M^2 p_u \left(\sum_{l=0}^{L-1} \sigma_{hkl}^2 \right)^2 e^{-\sigma_{\omega_k}^2 (t-(k-1)L)^2}$
$\text{SIF}_k[t]$	$\mathbb{E}[\text{SIF}_k[t] ^2] = M^2 p_u \left[1 - e^{-\sigma_{\omega_k}^2 (t-(k-1)L)^2} \right] \left(\sum_{l=0}^{L-1} \sigma_{hkl}^2 \right)^2 + M p_u \sum_{l=0}^{L-1} \sigma_{hkl}^4$
$\text{ISI}_k[t]$	$\mathbb{E}[\text{ISI}_k[t] ^2] = M p_u \left[\left(\sum_{l=0}^{L-1} \sigma_{hkl}^2 \right)^2 - \sum_{l=0}^{L-1} \sigma_{hkl}^4 \right]$
$\text{MUI}_k[t]$	$\mathbb{E}[\text{MUI}_k[t] ^2] = M p_u \left(\sum_{l=0}^{L-1} \sigma_{hkl}^2 \right) \left(\sum_{q=1, q \neq k}^K \sum_{l=0}^{L-1} \sigma_{hql}^2 \right)$
$\text{EN}_k[t]$	$\mathbb{E}[\text{EN}_k[t] ^2] = \frac{M\sigma^2}{K} \left(\sum_{k=1}^K \sum_{l=0}^{L-1} \sigma_{hkl}^2 \right) + M\sigma^2 \left(\sum_{l=0}^{L-1} \sigma_{hkl}^2 \right) + \frac{M\sigma^4}{K p_u}$

Proposition 4. (*Achievable Information Rate*) Using the proposed coding strategy in Section V-A, an achievable information rate for the k^{th} UT, with $N_u =$ number of channel uses in an UL slot, is given by

$$I_k \triangleq \frac{1}{N_u} \sum_{t=KL+L-1}^{KL+N_D+L-2} \log_2(1 + \text{SINR}_k[t]), \quad \text{where,} \quad (40)$$

$$\text{SINR}_k[t] = \frac{M^2 p_u \left(\sum_{l=0}^{L-1} \sigma_{hkl}^2 \right)^2 e^{-\sigma_{\omega_k}^2 (t-(k-1)L)^2}}{M^2 p_u \left(1 - e^{-\sigma_{\omega_k}^2 (t-(k-1)L)^2} \right) \left(\sum_{l=0}^{L-1} \sigma_{hkl}^2 \right)^2 + M p_u \left(\sum_{l=0}^{L-1} \sigma_{hkl}^2 \right)^2 + M p_u \left(\sum_{l=0}^{L-1} \sigma_{hkl}^2 \right) \left(\sum_{q=1, q \neq k}^K \sum_{l=0}^{L-1} \sigma_{hql}^2 \right) + \frac{M\sigma^2}{K} \sum_{q=1}^K \sum_{l=0}^{L-1} \sigma_{hql}^2 + M\sigma^2 \sum_{l=0}^{L-1} \sigma_{hkl}^2 + \frac{M\sigma^4}{K p_u}}. \quad (41)$$

Proof: From the proposed coding strategy we know that each user has N_D channel codes (one for each of the N_D channel uses in an uplink data transmission block). A lower bound to the information rate of the t^{th} channel code is given by (38). So the average information rate for the k^{th} UT is lower bounded as

$$\frac{1}{N_u} \sum_{t=KL+L-1}^{KL+L+N_D-2} I(\hat{x}_k[t]; x_k[t]) \geq \frac{1}{N_u} \sum_{t=KL+L-1}^{KL+L+N_D-2} \log_2 \left(1 + \text{SINR}_k[t] \right) = I_k, \quad (42)$$

where we divide the sum by N_u to account for the fact that no information symbol is transmitted during the channel estimation, preamble and post-amble phases (see Fig. 1). From (38) we have

$$\text{SINR}_k[t] = \frac{\left| \mathbb{E} [A_k[t]] \right|^2}{\mathbb{E} [|W_k[t]|^2]} \stackrel{(a)}{=} \frac{\left| \mathbb{E} [A_k[t]] \right|^2}{\mathbb{E} [|\text{SIF}_k[t]|^2 + |\text{ISI}_k[t]|^2 + |\text{MUI}_k[t]|^2 + |\text{EN}_k[t]|^2]} \quad (43)$$

where (a) follows from the fact that the terms $\text{SIF}_k[t]$, $\text{ISI}_k[t]$, $\text{MUI}_k[t]$ and $\text{EN}_k[t]$ are zero mean and uncorrelated. Substituting the expressions from Table I in (43) we get (41). Since the expression on the R.H.S. in (42) is a lower bound to the average information rate, it is indeed an achievable rate for the k^{th} UT, as given in (40). ■

Remark 12. From (41) using $t_1 \triangleq t - (k-1)L$, $\theta_k \triangleq \sum_{l=0}^{L-1} \sigma_{hkl}^2$ and $\gamma_k = \frac{p_u}{\sigma^2} \theta_k$ we have

$$\text{SINR}_k[t] = \frac{M\gamma_k e^{-\sigma_{\omega_k}^2 t_1^2}}{M\gamma_k [1 - e^{-\sigma_{\omega_k}^2 t_1^2}] + c_1\gamma_k + \frac{1}{K\gamma_k} + c_2} = \frac{\overbrace{e^{-\sigma_{\omega_k}^2 t_1^2}}^{\text{Residual CFO}}}{\underbrace{[1 - e^{-\sigma_{\omega_k}^2 t_1^2}] + \frac{c_1}{M}}_{\text{(MUI + ISI + SIF)}} + \underbrace{\frac{1}{MK\gamma_k^2} + \frac{c_2}{M\gamma_k}}_{\text{due to the Channel estimation error and AWGN}}}, \quad (44)$$

where $c_1 \triangleq \frac{1}{\theta_k} \sum_{q=1}^K \theta_q$ and $c_2 \triangleq \left(\frac{1}{K\theta_k} \sum_{q=1}^K \theta_q \right) + 1$. Clearly as $M \rightarrow \infty$, the MUI, ISI and SIF terms disappear. If we have $\gamma_k \propto 1/\sqrt{M}$, from Proposition 2 we know that the MSE $\sigma_{\omega_k}^2 = \mathbb{E}[(\hat{\omega}_k - \omega_k)^2]$ remains fixed as $M \rightarrow \infty$, i.e., the impact of the residual CFO on the SINR does not vary significantly as $M \rightarrow \infty$. In (44) we notice that the term $\left(\frac{1}{MK\gamma_k^2} + \frac{c_2}{M\gamma_k} \right)$ due to AWGN and channel estimation error depends on γ_k and therefore we must decrease γ_k in such a way that this term does not grow unbounded as $M \rightarrow \infty$. With decreasing $\gamma_k \rightarrow 0$, $\frac{1}{MK\gamma_k^2}$ would eventually dominate over $c_2/M\gamma_k$. Hence we should reduce γ_k at a rate equal to or slower than $1/\sqrt{M}$ with increasing M . This shows that an $\mathcal{O}(\sqrt{M})$ array gain is achievable with the proposed CFO estimation and compensation scheme. This is indeed true as we show it more rigorously in the following theorem. □

Theorem 2. (*Achievable Array Gain*) Consider $|\omega_k KL| \ll \pi$. For a fixed K , L , N , and a fixed desired information rate, $R_k[t] \gg R_0$ of the t^{th} channel code (where $R_0 \triangleq \log_2 \left(1 + \frac{2}{N-KL} \right)$), there exists a positive constant $c_0 > 0$ such that by decreasing $\gamma_k = \frac{c_0}{\sqrt{M}}$, with increasing M , we have

$$\lim_{M \rightarrow \infty} \log_2 \left(1 + \text{SINR}_k[t] \right) = R_k[t]. \quad (45)$$

Proof: See Appendix C. ■

Remark 13. From Theorem 2 it follows that for fixed K , L , N and a fixed desired achievable information rate, I_k for the k^{th} UT, the required received SNR γ_k decreases roughly by 1.5 dB with every doubling in M , i.e., an $\mathcal{O}(\sqrt{M})$ array gain. This observation is also supported

through Fig. 9. Previous works have reported an $\mathcal{O}(\sqrt{M})$ array gain in the presence of channel estimation errors only (i.e. no residual CFO) [8]. An important contribution of our work is that even in the presence of CFO the proposed CFO estimation and compensation technique does not degrade the array gain, which is still $\mathcal{O}(\sqrt{M})$. \square

VI. NUMERICAL RESULTS AND DISCUSSIONS

In all simulation studies presented in this section, we assume an operating carrier frequency $f_c = 2$ GHz and a maximum CFO of 0.1 PPM of f_c . We assume a communication bandwidth $B_w = 1$ MHz, the maximum delay spread is $T_d = 5\mu s$ and the coherence interval is $T_c = 1$ ms. Therefore $|\omega_k| \leq \frac{\pi}{2500}$ (see footnote 7 in *Remark 1*). At the start of every CFO estimation phase ω_k assumes a new value (independent of the previous values). This new value is uniformly distributed in the interval $\left[-\frac{\pi}{2500}, \frac{\pi}{2500}\right]$. From the proposed communication strategy in Section II (see Fig. 1), we have $N_c = T_c B_w = 1000$, $N = N_u = N_c/2 = 500$ and $L = T_d B_w = 5$ ($N_u =$ number of channel uses in the UL slot). The PDP is the same for each user and is given by $\sigma_{hkl}^2 = 1/L$, $l = 0, 1, \dots, L-1$, $k = 1, 2, \dots, K$. Subsequently for the first user (i.e. $k = 1$) we present the variation in the required SNR (to achieve a fixed desired per-user information rate) as a function of increasing M and N_D ($N_D =$ UL data transmission length). The observations and insights made in the following remain the same for any other user as well. Therefore without loss of generality we illustrate our results only for the first user.

In Fig. 9, for a fixed $N = N_u = 500$, $L = 5$, and $K = 10$ and a fixed desired achievable information rate for the first user (i.e. $I_k = 1$ bpcu and $I_k = 2$ bpcu for $k = 1$) we plot the numerically computed received SNR γ_k required to achieve I_k , as a function of increasing M . We

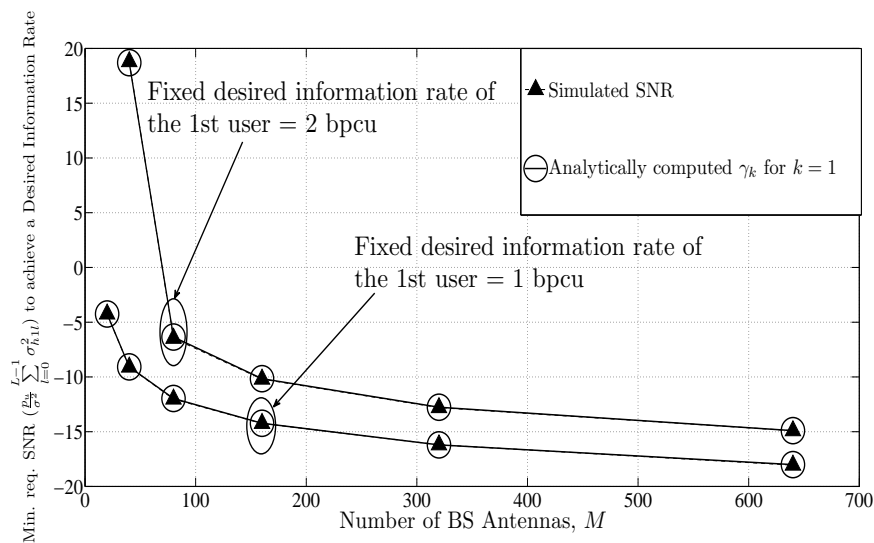


Fig. 9 Plot of the required received SNR γ_k to achieve a fixed rate I_k versus M , number of BS antennas.

also compute the required SNR γ_k analytically by using (40) and (41), with $\sigma_{\omega_k}^2 = \mathbb{E}[(\hat{\omega}_k - \omega_k)^2]$ replaced by its approximate expression in (15). Note that we use (15) with $G_k = 1$, since the expectation $\mathbb{E}[(\hat{\omega}_k - \omega_k)^2]$ is taken across multiple CFO estimation phases and also due to the fact that $G_k \rightarrow 1$ as $M \rightarrow \infty$ (see Remark 2). In Fig. 9 we observe that the analytical approximation to the minimum required SNR is indeed tight. Further for both $I_k = 1$ bpcu and $I_k = 2$ bpcu the required SNR decreases by roughly 1.5 dB as M increases from $M = 320$ to $M = 640$. This observation supports Theorem 2 and shows that an $\mathcal{O}(\sqrt{M})$ array gain is achievable.

In Fig. 10, we plot the variation in the information rate achieved by the first UT as a function of increasing N_D (UL data transmission length). We consider a fixed $K = 10$, $L = 5$ and $\gamma_k = -5$ dB. The length of the pilot sequence for CFO estimation, i.e., N , is same as the length of the UL block, i.e., $N = N_u = N_D + KL + 2(L - 1)$. We plot the information rate under the following scenarios: (i) ideal situation with no/zero CFO (solid curve without any marker); (ii) CFO present but no CFO estimation/compensation is performed (solid curve marked with filled triangles); (iii) CFO present with proposed CFO estimation/compensation. For the last scenario, we plot both the numerically simulated information rate (dashed curve marked with stars) and also the analytically computed value (solid curve marked with diamonds). The analytical value of the information rate is computed using (40) and (41). In (41), $\sigma_{\omega_k}^2 = \mathbb{E}[(\hat{\omega}_k - \omega_k)^2]$ is replaced by the expression on the R.H.S. in (15) with $G_k = 1$. For both $M = 40$ and $M = 160$, it is observed that if no CFO estimation/compensation is performed, the information rate decreases rapidly with increasing N_D .

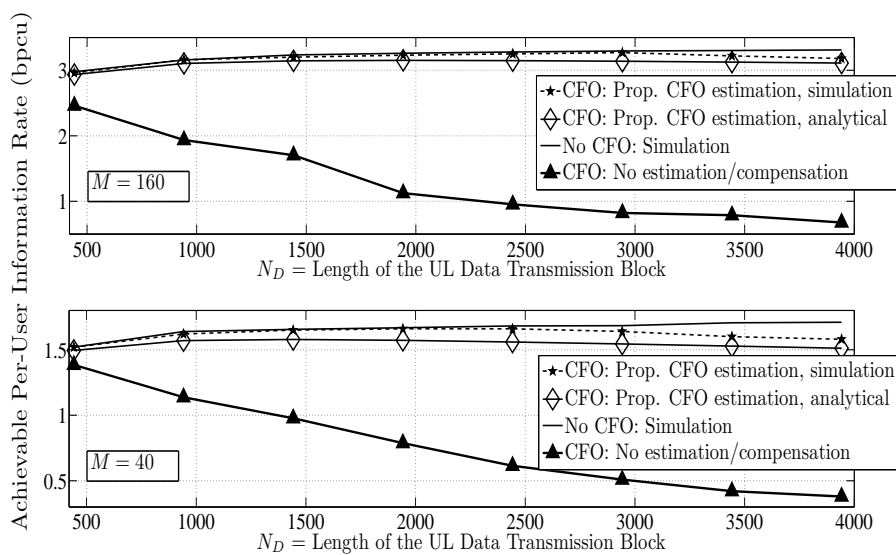


Fig. 10 Plot of the information rate of the first user versus N_D , with fixed $M = 40, 160$, $K = 10$, $L = 5$ and SNR $\gamma_k = -5$ dB.

This is expected since with increasing N_D , the channel estimates used for coherent detection at the BS become stale (i.e. due to the CFO, the phase error between the channel estimate and the channel gain in the received information signal increases with increasing time lag between the channel estimation phase and the time instance when the information symbol is received).

However with the proposed CFO estimation/compensation, the information rate is nearly the same as the rate when no CFO is present (ideal situation). This is observed to be true for large N_D also (see Fig. 10). Therefore it follows that the proposed CFO estimation algorithm results in sufficiently small residual CFO, which does not result in a significant phase error between the channel estimate and the channel gain during coherent detection.

VII. POSSIBLE EXTENSIONS

In this section, we discuss some possible extensions to the work done in this paper.

- **Analytical Derivation of Near-optimality of the Proposed Algorithm-** In this paper, we have shown the near-optimality of the proposed CFO estimation algorithm numerically (see Fig. 5). It would be interesting to show the same analytically.
- **Alternative low PAPR pilot sequence for CFO Estimation-** The proposed pilot sequence for CFO estimation has zeros which could lead to a high PAPR (peak-to-average-power-ratio) of the pilot signals. Since high PAPR impacts the efficiency of the power amplifiers, an interesting direction is to find an alternative low-PAPR sequence which performs similar to or better than the proposed pilot sequence.
- **Study of the feedback mechanism for CFO compensation-** In the CFO compensation phase of the proposed communication strategy, we assume that the feedback is error free. It would be interesting to study the exact mechanism of this feedback and the impact of feedback errors.

APPENDIX A

PROOF OF LEMMA 1

From (9) we have

$$\nu_k^I \triangleq \Re(\nu_k) = \frac{1}{MKL(B-1)p_u \sum_{l=0}^{L-1} \sigma_{hkl}^2} \Re\{V_k\}, \text{ and } \nu_k^Q \triangleq \Im(\nu_k) = \frac{1}{MKL(B-1)p_u \sum_{l=0}^{L-1} \sigma_{hkl}^2} \Im\{V_k\}, \quad (46)$$

where $V_k \triangleq \sum_{b=1}^{B-1} \sum_{m=1}^M \sum_{l=0}^{L-1} c_k(b, m, l)$ and $c_k(b, m, l)$ is defined in (7). Since $n_m[t], \forall t$, are all complex circular symmetric, i.i.d. Gaussian, we have $\mathbb{E}[T_i] = 0, i = 1, 2, 3$ (T_i are defined in (7)). Therefore we have $\mathbb{E}[c_k(b, m, l)] = \sum_{i=1}^3 \mathbb{E}[T_i] = 0, \forall b = 1, 2, \dots, B-1, l = 0, 1, \dots, L-1$ and $m = 1, 2, \dots, M$.

Clearly, $\mathbb{E}[V_k] = \sum_{b=1}^{B-1} \sum_{m=1}^M \sum_{l=0}^{L-1} \mathbb{E}[c_k(b, m, l)] = 0$. Therefore from (46), it follows that $\mathbb{E}[\nu_k^I] = \mathbb{E}[\nu_k^Q] = 0$ and hence $\mathbb{E}[\nu_k] = 0$. The real components of T_i , $i = 1, 2, 3$ are given by

$$\begin{aligned} \Re(T_1) &= \sqrt{KLp_u} |h_{km}[l]| |n_m[\tau(b+1, k, l)]| \cos\left(\angle n_m[\tau(b+1, k, l)] - \angle h_{km}[l] - \omega_k \tau(b, k, l)\right), \\ \Re(T_2) &= \sqrt{KLp_u} |h_{km}[l]| |n_m[\tau(b, k, l)]| \cos\left(-\angle n_m[\tau(b, k, l)] + \angle h_{km}[l] + \omega_k \tau(b+1, k, l)\right), \\ \text{and } \Re(T_3) &= |n_m[\tau(b, k, l)]| |n_m[\tau(b+1, k, l)]| \cos\left(\angle n_m[\tau(b+1, k, l)] - \angle n_m[\tau(b, k, l)]\right), \end{aligned} \quad (47)$$

where $\angle c$ represents the ‘principal argument’ of $c \in \mathbb{C}$. Using expressions in (47), the variance of $\Re(V_k)$ is given by

$$\begin{aligned} \mathbb{E}[(\Re(V_k))^2] &= \mathbb{E}\left[\left(\sum_{b=1}^{B-1} \sum_{m=1}^M \sum_{l=0}^{L-1} \Re(T_1+T_2+T_3)\right)^2\right] = \sum_{b=1}^{B-1} \sum_{m=1}^M \sum_{l=0}^{L-1} \left[KLp_u |h_{km}[l]|^2 \sigma^2 \left\{ \mathbb{E}\left[\cos^2\left(\omega_k \tau(b+1, k, l) + \angle h_{km}[l] - \angle n_m[\tau(b, k, l)]\right)\right] \right. \right. \\ &+ \mathbb{E}\left[\cos^2\left(\angle n_m[\tau(b+1, k, l)] - \omega_k \tau(b, k, l) - \angle h_{km}[l]\right)\right] \left. \left. + \sigma^4 \mathbb{E}\left[\cos^2\left(\angle n_m[\tau(b+1, k, l)] - \angle n_m[\tau(b, k, l)]\right)\right] \right\} \right. \\ &+ 2 \sum_{b=2}^{B-1} \sum_{m=1}^M \sum_{l=0}^{L-1} \left\{ KLp_u |h_{km}[l]|^2 \sigma^2 \mathbb{E}\left[\cos\left(\angle n_m[\tau(b+1, k, l)] - \angle h_{km}[l] - \omega_k \tau(b+2, k, l)\right) \cos\left(\angle n_m[\tau(b+1, k, l)] - \angle h_{km}[l] - \omega_k \tau(b, k, l)\right)\right] \right\} \left. \right] \\ &= \sum_{b=1}^{B-1} \sum_{m=1}^M \sum_{l=0}^{L-1} \left\{ KLp_u |h_{km}[l]|^2 \sigma^2 + \sigma^4/2 \right\} + \sum_{b=2}^{B-1} \sum_{m=1}^M \sum_{l=0}^{L-1} \left\{ KLp_u |h_{km}[l]|^2 \sigma^2 \cos(2\omega_k KL) \right\}. \end{aligned} \quad (48)$$

Using the expression for $\mathbb{E}[(\Re(V_k))^2]$ from (48) and the expression for ν_k^I from (46), the variance of ν_k^I is given by (12). In similar fashion, we can show that the variance of ν_k^Q is given by (13). \square

APPENDIX B

PROOF OF THEOREM 1

With $\nu_k^I \triangleq \Re(\nu_k)$ and $\nu_k^Q \triangleq \Im(\nu_k)$, from (8) we get

$$\arg(\rho_k) = \tan^{-1} \left[\frac{G_k \sin(\omega_k KL) + \nu_k^Q}{G_k \cos(\omega_k KL) + \nu_k^I} \right]. \quad (49)$$

Note that $|\omega_k KL| \ll \pi \implies \cos(\omega_k KL) \approx 1$. Using this approximation in (12), we get

$$\frac{\mathbb{E}[(\nu_k^I)^2]}{G_k^2} \approx \frac{(2B-3)G_k}{(B-1)\gamma_k} + \frac{1}{2K\gamma_k^2} \stackrel{(a)}{\ll} 1, \quad (50)$$

where (a) follows from $\gamma_k \gg \gamma_k^0$. Therefore we conclude that ν_k^I/G_k is small (i.e., $\frac{\nu_k^I}{G_k} \ll 1$) with high probability. Using this approximation, we can write $G_k \cos(\omega_k KL) + \nu_k^I \approx G_k \cos(\omega_k KL)$.

Since $\mathbb{E}[(\nu_k^Q)^2] < \mathbb{E}[(\nu_k^I)^2]$ (compare (12) and (13) with the approximation $\cos(\omega_k KL) \approx 1$), we can also say that $\frac{\nu_k^Q}{G_k} \ll 1$ with high probability. Using above approximations in (49), we get

$$\begin{aligned} \arg(\rho_k) &\approx \tan^{-1} \left[\tan(\omega_k KL) + \frac{\nu_k^Q}{G_k \cos(\omega_k KL)} \right] \stackrel{(a)}{\approx} \tan^{-1} \left[\tan(\omega_k KL) + \frac{\nu_k^Q}{G_k} \right] \\ &\stackrel{(b)}{\approx} \tan^{-1} \left[\frac{\tan(\omega_k KL) + \tan\left(\frac{\nu_k^Q}{G_k}\right)}{1 - \tan(\omega_k KL) \tan\left(\frac{\nu_k^Q}{G_k}\right)} \right] \stackrel{(c)}{\approx} \tan^{-1} \left[\tan\left(\omega_k KL + \frac{\nu_k^Q}{G_k}\right) \right] = \omega_k KL + \frac{\nu_k^Q}{G_k}, \end{aligned} \quad (51)$$

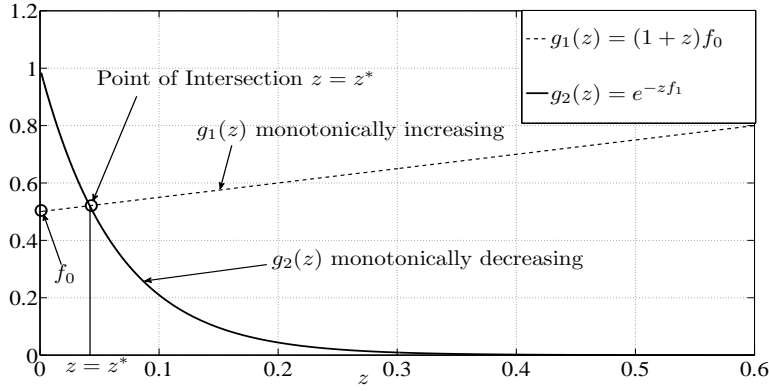


Fig. 11 Plot of $g_1(z)$ and $g_2(z)$ showing their unique point of intersection as the solution to (53).

where (a) follows from substituting $\cos(\omega_k KL) \approx 1$. Step (b) follows from the fact that since $\frac{\nu_k^Q}{G_k} \ll 1$ with high probability, $\frac{\nu_k^Q}{G_k} \approx \tan(\frac{\nu_k^Q}{G_k})$ and $|\tan(\omega_k KL) \tan(\frac{\nu_k^Q}{G_k})| \ll 1$ with high probability. Step (c) follows from the standard result $\tan(A+B) = (\tan A + \tan B)/(1 - \tan A \tan B)$. Substituting (51) in (10), we get the desired approximation for the CFO estimate in (14). \square

APPENDIX C

PROOF OF THEOREM 2

From (44) we explicitly rewrite $\text{SINR}_k[t]$ as a function of M since N , K and L are fixed and M is varying, i.e.,

$$\text{SINR}_{k,M}[t] = \frac{e^{-\sigma_{\omega_k}^2 t_1^2}}{\left[1 - e^{-\sigma_{\omega_k}^2 t_1^2}\right] + \frac{c_1}{M} + \frac{1}{MK\gamma_k^2} + \frac{c_2}{M\gamma_k}}, \quad (52)$$

where $c_1 \triangleq \frac{1}{\theta_k} \sum_{q=1}^K \theta_q$, $c_2 \triangleq \left(\frac{1}{K\theta_k} \sum_{q=1}^K \theta_q\right) + 1$, $\theta_k = \sum_{l=0}^{L-1} \sigma_{h_{kl}}^2$ and $t_1 = t - (k-1)L$. Let K , L , N and $R_k[t]$ be fixed as $M \rightarrow \infty$. Let $\gamma_k \triangleq \frac{c_0}{\sqrt{M}}$, where c_0 is such that $u = c_0 > 0$ is the unique solution to

$$\left(1 + \frac{1}{Ku^2}\right) \left(1 - 2^{-R_k[t]}\right) = e^{-t_1^2/2Ku^2d'}, \quad \text{where } d' \triangleq (N - KL)(KL)^2. \quad (53)$$

The uniqueness of the constant c_0 is argued in the following. Let $z \triangleq \frac{1}{Ku^2}$. Then (53) is equivalent to

$$(1+z)f_0 = e^{-zf_1}, \quad \text{where } f_0 \triangleq 1 - 2^{-R_k[t]}, \quad \text{and } f_1 \triangleq \frac{t_1^2}{2d'}. \quad (54)$$

Note that both f_0 and f_1 are positive, i.e., $f_0 > 0$, $f_1 > 0$ and $0 < f_0 < 1$. In (54) the R.H.S. $g_2(z) \triangleq e^{-zf_1}$ is monotonically decreasing with increasing z and the L.H.S. $g_1(z) \triangleq (1+z)f_0$ is monotonically increasing with increasing z . Also at $z = 0$, $g_2(z = 0) = 1 > g_1(z = 0) = f_0$, since $f_0 < 1$. The curves $g_1(z)$ and $g_2(z)$ therefore intersect at exactly one point, $z = z^* \triangleq \frac{1}{Kc_0^2}$, as is illustrated through Fig. 11.

With $u = c_0$ in (53) it follows that

$$R_k[t] = \log_2 \left(1 + \frac{e^{-t_1^2/2Kc_0^2d'}}{1 + \frac{1}{Kc_0^2} - e^{-t_1^2/2Kc_0^2d'}} \right). \quad (55)$$

We next show that $c_0 > \sqrt{\frac{2^{R_k[t]} - 1}{K}}$. In Fig. 11 we observe that since $g_2(z)$ is monotonically decreasing, and $g_2(z = 0) = 1$, it follows that $g_2(z = \frac{1}{Kc_0^2}) < 1$. Since $g_1(z = \frac{1}{Kc_0^2}) = g_2(z = \frac{1}{Kc_0^2})$, it follows that

$$g_1(z = \frac{1}{Kc_0^2}) = (1 + \frac{1}{Kc_0^2})(1 - 2^{-R_k[t]}) < 1 \implies \frac{1}{Kc_0^2} < \frac{1}{2^{R_k[t]} - 1} \implies c_0 > \sqrt{\frac{2^{R_k[t]} - 1}{K}}. \quad (56)$$

From (56) we have

$$\gamma_k = \frac{c_0}{\sqrt{M}} > \sqrt{\frac{2^{R_k[t]} - 1}{MK}} \stackrel{(a)}{\gg} \sqrt{\frac{2^{R_0} - 1}{MK}} = \sqrt{\frac{2}{MK(N - KL)}}, \quad (57)$$

where (a) follows from the fact that $R_k[t] \gg R_0 = \log_2 \left(1 + \frac{2}{N - KL} \right)$. Further we have

$$\gamma_k^0 \stackrel{(a)}{=} \frac{\frac{B-1}{2B-3}}{KG_k \left[\sqrt{1 + 2ML \frac{(B-1)^3}{(2B-3)^2}} - 1 \right]} \stackrel{(b)}{\leq} \frac{2 \frac{B-1}{2B-3}}{KG_k \sqrt{2ML \frac{(B-1)^3}{(2B-3)^2}}} = \sqrt{\frac{2}{MK(N - KL)}}. \quad (58)$$

Here, step (a) follows from the definition of γ_k^0 in Theorem 1 and (b) is obtained using the inequality $\sqrt{1+x} - 1 \geq \sqrt{x}/2$, $\forall x \geq 16/9$ with $x = 2ML \frac{(B-1)^3}{(2B-3)^2}$ (since $ML > 1$, $x = 2ML \frac{(B-1)^3}{(2B-3)^2} > \frac{16}{9}$). From (57) and (58) we finally have $\gamma_k = \frac{c_0}{\sqrt{M}} \gg \gamma_k^0$.

Since $|\omega_k KL| \ll \pi$ and $\gamma_k \gg \gamma_k^0$, using the Corollary to Theorem 1 we get

$$\sigma_{\omega_k}^2 = \mathbb{E}[(\hat{\omega}_k - \omega_k)^2] \stackrel{(a)}{\approx} \frac{1}{Md'} \left(\frac{1}{B-1} + \frac{1}{2K\gamma_k^2} \right), \quad (59)$$

where (a) follows from the fact that as $M \rightarrow \infty$, $G_k \rightarrow 1$ (see Remark 2). Substituting the expression of $\sigma_{\omega_k}^2$ from (59) and $\gamma_k = \frac{c_0}{\sqrt{M}}$ in (52) and taking the limit $M \rightarrow \infty$, we get

$$\begin{aligned} \lim_{M \rightarrow \infty} \log_2(1 + \text{SINR}_{k,M}[t]) &= \log_2 \left(1 + \lim_{M \rightarrow \infty} \frac{e^{-t_1^2 \left(\frac{1}{2Kc_0^2d'} + \frac{1}{d'(B-1)\sqrt{M}} \right)}}{\left[1 - e^{-t_1^2 \left(\frac{1}{2Kc_0^2d'} + \frac{1}{d'(B-1)\sqrt{M}} \right)} \right] + \frac{c_1}{M} + \frac{1}{Kc_0^2} + \frac{c_2}{c_0\sqrt{M}}} \right) \\ &= \log_2 \left(1 + \frac{e^{-t_1^2/2Kc_0^2d'}}{1 + \frac{1}{Kc_0^2} - e^{-t_1^2/2Kc_0^2d'}} \right) \stackrel{(a)}{=} R_k[t], \end{aligned} \quad (60)$$

where (a) follows from (55). \square

REFERENCES

- [1] A. Fehske, G. Fettweis, J. Malmudin, and G. Biczok, "The Global Footprint of Mobile Communications: The Ecological and Economic Perspective," *IEEE Commun. Mag.*, vol. 49, no. 8, pp. 55–62, August 2011.
- [2] J. Andrews, S. Buzzi, W. Choi, S. Hanly, A. Lozano, A. Soong, and J. Zhang, "What Will 5G Be?" *IEEE J. Sel. Areas Commun.*, vol. 32, no. 6, pp. 1065–1082, June 2014.
- [3] F. Boccardi, R. Heath, A. Lozano, T. Marzetta, and P. Popovski, "Five Disruptive Technology Directions for 5G," *IEEE Commun. Mag.*, vol. 52, no. 2, pp. 74–80, February 2014.
- [4] T. Marzetta, "Noncooperative Cellular Wireless with Unlimited Numbers of Base Station Antennas," *IEEE Trans. Wireless Commun.*, vol. 9, no. 11, pp. 3590–3600, November 2010.
- [5] F. Rusek, D. Persson, B. K. Lau, E. Larsson, T. Marzetta, O. Edfors, and F. Tufvesson, "Scaling Up MIMO: Opportunities and Challenges with Very Large Arrays," *IEEE Signal Process. Mag.*, vol. 30, no. 1, pp. 40–60, Jan 2013.
- [6] E. Larsson, O. Edfors, F. Tufvesson, and T. Marzetta, "Massive MIMO for Next Generation Wireless Systems," *IEEE Commun. Mag.*, vol. 52, no. 2, pp. 186–195, February 2014.
- [7] H. Q. Ngo, E. Larsson, and T. Marzetta, "Uplink Power Efficiency of Multiuser MIMO with Very Large Antenna Arrays," in *Communication, Control, and Computing (Allerton), 2011 49th Annual Allerton Conference on*, Sept 2011, pp. 1272–1279.
- [8] —, "Energy and Spectral Efficiency of Very Large Multiuser MIMO Systems," *IEEE Trans. Commun.*, vol. 61, no. 4, pp. 1436–1449, April 2013.
- [9] P. Stoica and O. Besson, "Training Sequence Design for Frequency Offset and Frequency-Selective Channel Estimation," *IEEE Trans. Commun.*, vol. 51, no. 11, pp. 1910–1917, Nov 2003.
- [10] O. Besson and P. Stoica, "On Parameter Estimation of MIMO Flat-Fading Channels with Frequency Offsets," *IEEE Trans. Signal Process.*, vol. 51, no. 3, pp. 602–613, March 2003.
- [11] J. Chen, Y.-C. Wu, S. Ma, and T.-S. Ng, "Joint CFO and Channel Estimation for Multiuser MIMO-OFDM Systems with Optimal Training Sequences," *IEEE Trans. Signal Process.*, vol. 56, no. 8, pp. 4008–4019, Aug 2008.
- [12] E. P. Simon, L. Ros, H. Hijazi, and M. Ghogho, "Joint Carrier Frequency Offset and Channel Estimation for OFDM Systems via the EM Algorithm in the Presence of Very High Mobility," *IEEE Trans. Signal Process.*, vol. 60, no. 2, pp. 754–765, Feb 2012.
- [13] M. Ghogho and A. Swami, "Training Design for Multipath Channel and Frequency-Offset Estimation in MIMO Systems," *IEEE Trans. Signal Process.*, vol. 54, no. 10, pp. 3957–3965, Oct 2006.
- [14] Y. Yu, A. Petropulu, H. Poor, and V. Koivunen, "Blind Estimation of Multiple Carrier Frequency Offsets," in *Personal, Indoor and Mobile Radio Communications, 2007. PIMRC 2007. IEEE 18th Intl. Symp. on*, Sept 2007, pp. 1–5.
- [15] H. Cheng and E. Larsson, "Some Fundamental Limits on Frequency Synchronization in massive MIMO," in *Signals, Systems and Computers, 2013 Asilomar Conference on*, Nov 2013, pp. 1213–1217.
- [16] A. Pitarokoilis, S. Mohammed, and E. Larsson, "Uplink Performance of Time-Reversal MRC in Massive MIMO Systems Subject to Phase Noise," *IEEE Trans. Wireless Commun.*, vol. 14, no. 2, pp. 711–723, Feb 2015.
- [17] S. Mukherjee and S. K. Mohammed, "Low-Complexity CFO Estimation for Multi-User Massive MIMO Systems," submitted to *IEEE Globecom, 2015* [Online]. Available: <http://arxiv.org/abs/1504.05657v2>.
- [18] M. Weiss, "Telecom Requirements for Time and Frequency Synchronization,," National Institute of Standards and Technology (NIST), USA, [Online]: www.gps.gov/cgsic/meetings/2012/weiss1.pdf.
- [19] U. DOETSCH and M. Ohm, "Apparatus, method and computer program for determining a frequency offset," Dec. 2013, uS Patent App. 14/000,021. [Online]. Available: <http://www.google.com/patents/US20130329721>
- [20] B. Hassibi and B. Hochwald, "How Much Training is Needed in Multiple-Antenna Wireless Links?" *IEEE Trans. Inf. Theory*, vol. 49, no. 4, pp. 951–963, April 2003.